

COMPUTATIONAL MODELING AND ANALYSIS OF FACE PROFILE OF PISTON RING

A DISSERTATION

SUBMITTED IN PARTIAL FULFILLMENT OF THE REQUIREMENTS FOR THE AWARD
OF THE DEGREE OF

MASTER OF TECHNOLOGY

IN

COMPUTATIONAL DESIGN

Submitted by:

AWANTIKA MISHRA

(2K16/CDN/02)

Under the supervision of

Prof. R.C. SINGH



DEPARTMENT OF MECHANICAL ENGINEERING

DELHI TECHNOLOGICAL UNIVERSITY

(Formerly Delhi College of Engineering)

Bawana Road, Delhi-110042

JULY, 2018



DELHI TECHNOLOGICAL UNIVERSITY

(Formerly Delhi College of Engineering)

Bawana Road, Delhi-110042

CANDIDATE'S DECLARATION

I, Awantika Mishra, Roll No. 2k16/CDN/02, student of M.Tech (Computational Design), hereby declare that the Major Project-II dissertation titled “Computational modeling and analysis of face profile of piston ring” which is submitted by me to the Department of Mechanical Engineering, Delhi Technological University, Delhi in partial fulfillment of the requirement for the award of the degree of Master of Technology in Computational Design under the supervision of Prof. R. C. Singh, is original and not copied from any source without any proper citation. This work has not previously formed the basis for the award of any Degree, Diploma Associateship, Fellowship or other similar title or recognition.

Place: Delhi

(AWANTIKA MISHRA)

Date:

Roll No. 2K16/CDN/02



DEPARTMENT OF MECHANICAL ENGINEERING

DELHI TECHNOLOGICAL UNIVERSITY

(Formerly Delhi College of Engineering)

Bawana Road, Delhi-110042

CERTIFICATE

I hereby certify that the Major Project-II dissertation titled “Computational modeling and analysis of face profile of piston ring” which is submitted by Ms Awantika Mishra, Roll No 2K16/CDN/02 in the Department of Mechanical Engineering of Delhi Technological University, Delhi in partial fulfillment of the requirement for the award of the degree of Master of Technology in Computational Design, is a record of the project work carried out by the her under my supervision. To the best of my knowledge and belief this work has not been submitted in part or full for the award of any Degree or Diploma to this University or elsewhere.

Place: Delhi

(Prof. R.C Singh)

Date:

Mechanical Engineering Department

Delhi Technological University, Delhi

ACKNOWLEDGEMENTS

First and foremost, praises and thanks to the God, the Almighty, for his showers of blessings throughout my research work to complete the research successfully.

I found my pen incompetent to express my thanks to my supervisor **Dr. Ramesh Chandra Singh Professor, DTU** under his kind and worthy guidance and supervision; I had the opportunity to carry out this work. It was only due to his advice, thoughtful comments, constructive criticism, and continuous vigilance over the progress of my work with a personal interest that it has taken this shape. He has been a great source of encouragement. To get an opportunity to carry out the project work in the well-equipped, ever developing laboratories in our institution, I would like to pay my deep sense of thankfulness to **Prof. Vipin, HOD, Department of Mechanical Engineering, DTU.**

I am very much thankful to my parents and sister for their moral support and encouragement, which was giving me the strength to chase my goal. Without their support and inspiration, I would not be able to complete my degree.

I would especially like to acknowledge my gratitude to all my dear friends for their consistent support, valuable suggestions from time to time to make this project worthy.

With a silent prayer to the Almighty, I take this opportunity to express my gratitude to all those who have supported me in completing my fourth-semester project work as a part of my degree program.

AWANTIKA MISHRA
M. Tech. (COMPUTATIONAL DESIGN)
2K16/CDN/02

ABSTRACT

The engine is one of the most widely used machines in today's era, which consists of a number of components, many of which can be accounted as tribological pairs such as bearings, transmissions, gears, pistons, clutches, wiper blades, tires, and electrical contacts that accounts to frictional power losses. A substantial portion of these frictional losses (20-40% approximately) is attributed to the piston-ring liner assembly. The tribological and computational study can reduce frictional losses to some extent which provide saving in fuel consumption and increase the engine life.

In this project, one dimensional analysis for the lubrication of the piston ring and cylinder liner has been developed. The piston ring has been treated as a reciprocating, dynamically-loaded bearing with a combined squeeze and sliding motion. Again combined elliptical-parabolic profile has been developed of the piston ring and modeled for face profile of piston ring. Equations have been developed for the face profile through MATLAB coding. The profile of the piston ring along width was more prominent for forming fluid film thickness.

A numerical procedure was developed to obtain the cyclic variations of fluid film thickness with the crank angle. Also, it was further utilized to determine the hydro-dynamic fluid film pressure over the span of the piston ring.

TABLE OF CONTENTS

CANDLDATE'S DECLARATION	ii
CERTIFICATE	iii
ACKNOWLEDGEMENTS	iv
ABSTRACT.....	v
TABLE OF CONTENTS.....	vi
LIST OF FIGURES	viii
LIST OF NOMENCLATURE	ix
CHAPTER 1: INTRODUCTION	1
1.1.1 TRIBOLOGY: MEANING AND APPLICATIONS.....	1
1.1.1 TRIBOLOGY: A SHORT HISTORY	2
1.2 CONSEQUENCES OF FRICTION ON IC ENGINE	4
1.3 LUBRICATION MECHANISMS	6
1.4 STRIBECK CURVE.....	7
1.5 WEAR.....	8
1.6 PISTON RING AND CYLINDER LINER	11
1.6.1 PISTON.....	11
1.6.2 PISTON RINGS CLASSIFICATION	12
1.6.3 CYLINDER LINER.....	13
CHAPTER 2: LITERATURE REVIEW	16
CHAPTER 3: THEORETICAL MODEL.....	26
3.1 FORCES ACTING ON PISTON RING.....	26
3.1.1 FORCES ON THE PISTON RING DURING THE AXIAL MOVEMENT.....	27
3.1.2 FORCES ON PISTON RING DURING RADIAL MOVEMENT	28
3.2 REYNOLD'S EQUATION	28
CHAPTER 4: RESULTS AND DISCUSSIONS.....	39
4.1 OIL FILM THICKNESS V/S CRANK ANGLE.....	39
4.2 PRESSURE V/S CRANK ANGLE DIAGRAM	40
CHAPTER 5: CONCLUSIONS AND FUTURE ASPECT	42

5.1 CONCLUSIONS.....	42
5.2 FUTURE ASPECT:.....	43
REFERENCES.....	44
APPENDIX 1.....	47
APPENDIX 2.....	51

LIST OF FIGURES

Fig. No.	Title	Page No.
1.1	Objectives of Tribology	2
1.2	Energy Distribution in the IC engine	4
1.3	Distribution of Mechanical Losses in IC engine	5
1.4	Types of Lubrication	7
1.5	Stribeck curve distinguishes lubrication regimes of engine components	8
1.6	Adhesion Wear	8
1.7	Fatigue Wear	9
1.8	Abrasive Wear	10
1.9	Erosive Wear	10
1.10	Corrosive Wear	11
1.11	Piston Ring	12
1.12	Compression Rings and Oil Scrapper Rings	13
1.13	Heat transfer in the piston ring and liner assembly	14
1.14	Leak proof Cylinder liner	14
1.15	Blow By problem in IC engine	15
3.1	Tilting in piston ring	26
3.2	Forces acting on piston ring	27
3.3	Model of Parabolically worn out piston ring face profile	29
3.4	Worn out piston ring face profile- Parabolic	31
3.5	Model of Elliptically worn out piston ring face profile	32
3.6	Worn out piston ring face profile- Elliptical	34
3.7	Model of Parabolic and elliptical profile on the same geometry	35
3.8	Combining worn out piston ring face profile- Elliptical+Parabolic	35

3.9	model of piston ring combined face profile	37
3.10	Complete worn piston ring profile	37
4.1	Predicted Cyclic Variation of Minimum Film Thickness	39
4.2	Variation of pressure v/s Width of the piston ring	40
4.3	Variation of pressure with piston ring width – Reynold’s Condition	41

LIST OF TABLES

Table No.	Title	Page no.
1	Historical achievement of Tribology.	3

LIST OF NOMENCLATURE

c = distance between the point of minimum oil film thickness to the end point of the profile.

h_{min} = minimum oil film thickness

P = pressure intensity

θ = crank angle

h = oil film thickness

U = Maximum velocity of piston

u = Instantaneous velocity of piston

r = crank radius

n = ratio of connecting rod length to crank radius

τ = Shear stress

ρ = Density of oil

b = width of piston ring

N = Speed of engine

x = axial distance

z = radial direction

t = tilting offset

o = offset distance

μ = microns

η = oil viscosity

F_{gas} = Gas pressure

F_{fric} = Frictional force

F_I = Inertial Force

F_{bend} = Bending Force

F_{hydr} = Hydrodynamic Force

$F_{contact}$ = Contact Force

$F_{tension}$ = Tension force

m_{ring} = mass of piston ring

\ddot{Y} = acceleration of piston ring in axial direction

CHAPTER 1: INTRODUCTION

1.1.1 TRIBOLOGY: MEANING AND APPLICATIONS

Tribology is the science of wear and tear, lubrication and friction, and however, includes interacting surfaces and alternative tribo-elements behave in relative motion in natural and artificial systems. Tribology focuses round the three parameters; friction, wear and lubrication of interacting surfaces in relative movement. It is the new field of science characterized in 1967 by the panel of the Association for the Economic Cooperation and Development. Tribology contains two Greek words: 'Tribos' which means rubbing or sliding and 'logos' meaning science.

Tribology is the field of science which applies an operational examination to issue of extraordinary economic significance such as reliability, maintenance, and wear of technical equipment ranging from household appliances to spacecraft. Wear is the significant reason for material wastage and loss of mechanical execution. Any decrease in the wear can spare significant measure of money and material. Friction is the primary driver of wear and energy scattering. It is evaluated that the 33% of the world's energy assets in display utilize is expected to beat the friction in shape or another. Lubrication turned out to be the successful methods for controlling the contact (friction).

A surface collaboration controls the working of each device accessible with surface contact. Each device made by a human is subjected to friction and wear which the consequence of the relative motion between the surfaces. Human body additionally has numerous interacting surfaces, e.g. knee joints, finger knuckles. Thus these parts likewise subjected to the lubrication and wear.

Tribology impacts the life of living creatures also and that to a greater degree. It is ordinarily observed that human skin moves toward becoming sweat-soaked when it senses fear or stress. It has been found that the sweat on the palms and sole of the feet can build the friction between palm or feet and the solid surface. This increase in friction is advantageous for people in the case of danger; the sweat helps to immovably hold the weapon or climb the closest tree.

The practical objective of mechanical engineering is to reduce the disadvantages of solid to solid contact; friction and wear. However, in some things, one need friction and wear to occur. There are measure cases wherever minimizing friction and maximizing wear or minimizing wear and maximizing friction or maximizing each friction and wear is desirable. For instance, reduction of wear, however not friction is desirable in brakes and greased clutches, reduction of friction however not wear is desirable in pencils, increase in each friction and wear is fascinating in erasers.

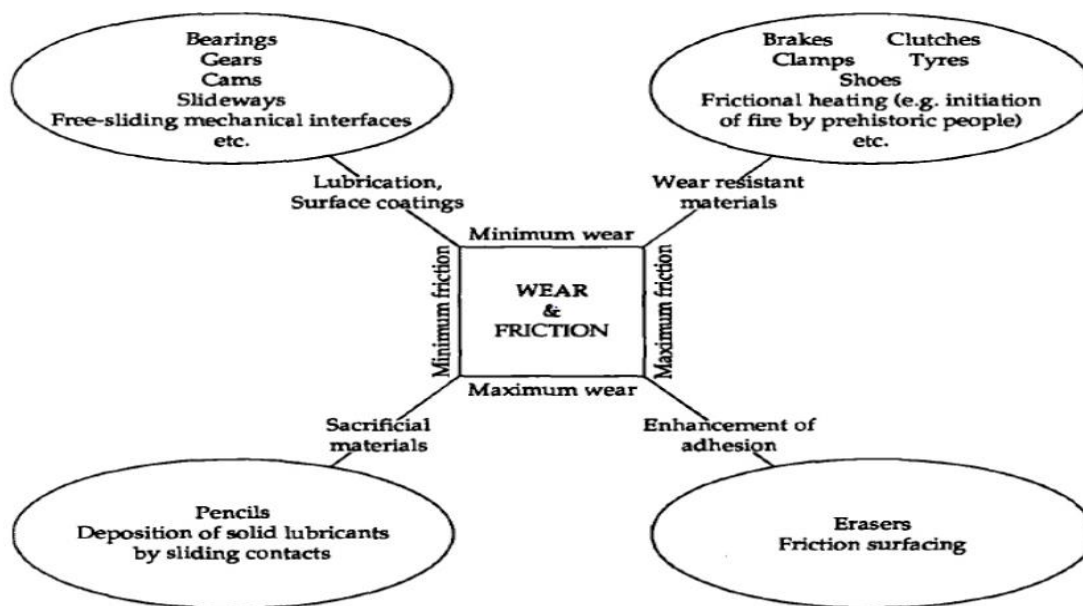


Fig 1.1: Objectives of Tribology [8]

1.1.1 TRIBOLOGY: A SHORT HISTORY

Tribological experiments prompt by Leonardo da Vinci Early history despite the comparatively recent naming of the sphere of mechanical engineering, quantitative studies of friction is copied as so much back as 1493, once Leonardo da Vinci initial noted the two elementary ‘laws’ of friction. According to da Vinci, frictional resistance was identical for two different completely different objects of identical weight, however, creating contact over different widths and lengths. He observed that the force required to overcome friction doubles as weight doubles.

The historical backdrop of any cutting edge science is regularly very rich. The authentic proof is found through archeological reality and incidental composed record. The historical backdrop of

tribology is not distinctive, with tribological accomplishments spreading over the time from the earliest starting point of humankind, to current.

1.1.3 EVOLVE OF TRIBOLOGY

The field of tribology is generally more critical and interdisciplinary. It was created in 1966 by British physicist David Tabor. The training and basic parts of tribology are very old. The root word "tribos" is interpreted from Greek to signify "rubbing" and numerous early imperative tribological perceptions were made by Greek logicians, researchers, and mechanics. For instance, in 400 B.C., Aristotle mentioned the objective fact in his work Questions Mechanicae that grinding was known as an extremely discernible constrain and least for round items. Table 1 underneath highlights a couple of the chronicled accomplishments in tribology related to this exploration.

Table 1: Accomplishments in tribology over the years

Tribologist	Achievement	Time Period
Early Mankind	Earliest use of friction in the conquest of fire through rubbing, drilling or percussion	1,000,000 – 11000 years ago
Egyptian Civilization	Transportation of 500 ton obelisks on sledges	2400 BC
Greek and Romans	Focus on philosophy and science by Greek and roman cultures, use of metal bearings and lubricant	900 BC- 400 AD
Leonardo da Vinci	Observation of proportionality of friction. Wear studies for the development of bearing materials. The invention of rolling element bearings.	1400-1600 AD
Guillaume Amontous Charles, Augustin Coulumb, Leonhard Euler	Development of Laws of Friction, Coefficient of friction.	1600-1750 AD
Heinrich Hertz	Development of elastic body contact theory	1881 AD

1.2 CONSEQUENCES OF FRICTION ON IC ENGINE

In the present time, Automobiles have turned into an indivisible piece of human life. Each uses automobiles for comfort voyaging, transportation of products, giving emergency services and so on. In this way, it turns into the obligation of the individuals to keep up the serviceability of the automobiles to a more drawn out timeframe.

There are numerous explanations for the low efficiency of the automobile. Energy loss from various areas causes the low thermal efficiency of the engine. It is seen by Taylor, in Fig. 1.2, around 65% of heat is transferred to the surrounding as heat from exhaust, lubrication, and coolant. Another 10% of the energy from the engine is lost as heat to the surrounding from the surfaces of the engine due to friction. After every one of these losses around 25% of energy is accessible for the brake power and transmission and subsequently at last after further losses in the transmission power is conveyed to the wheels.

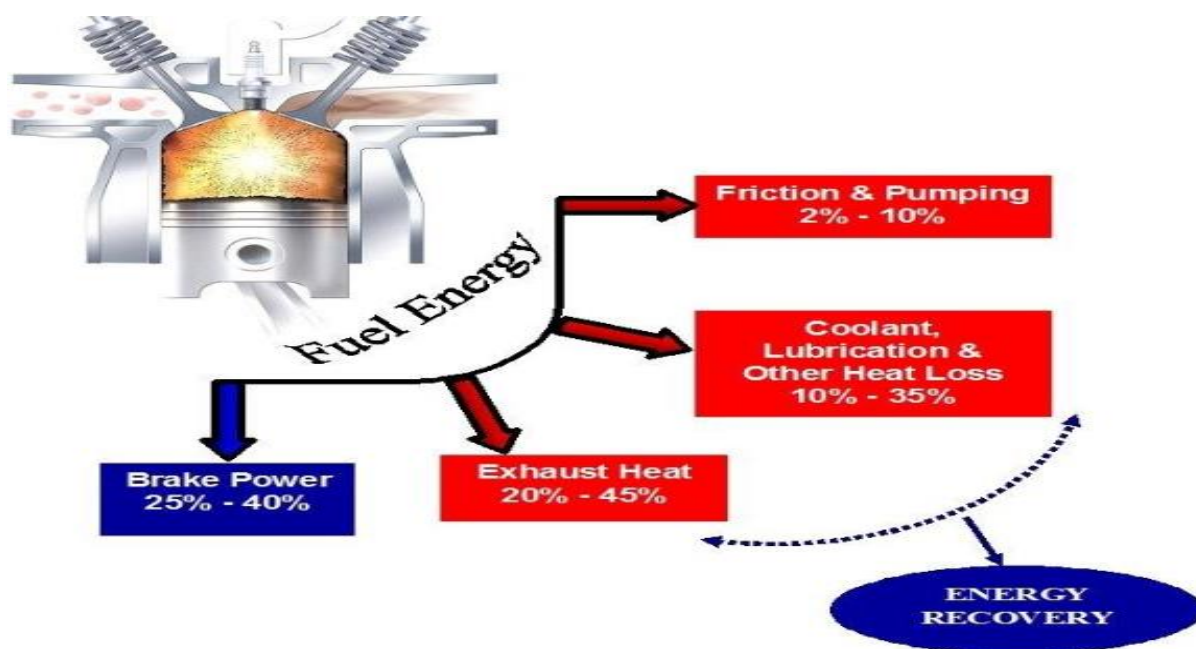


Fig 1.2: Energy Distribution in the IC engine [2].

Around 80% of the mechanical losses were related with the frictional components of the motor, i.e., valve prepare, piston congregations and bearings. There were additionally some

auxiliary losses which account for around 20% of the mechanical losses. The oil pump in the limiting engine speeds is to be less than 10% efficient and consume 2 to 3 kW. To reduce these losses in the engine one ought to need to do film oil examination alongside the different tribological aspects. In any case, one should also remember that the reliability and durability of the components must not be degraded to reduce these losses.

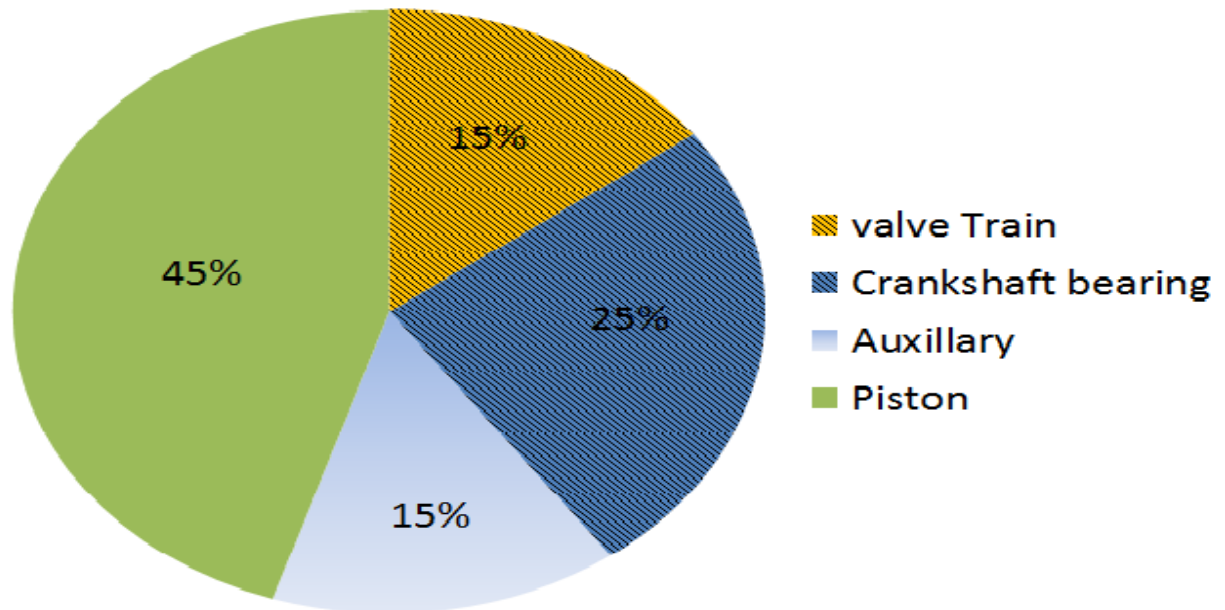


Fig 1.3: Distribution of Mechanical Losses in IC engine [2]

LUBRICATION

Lubrication is that the management of friction and wear by the introduction of a friction-reducing film between moving surfaces in grips. The lubricator used is often fluid, solid, or plastic substance. Lubrication is that the method or technique of employing a lubricator to reduce friction and/or wear in a very contact between two surfaces. The study of lubrication could be a discipline within the field of mechanical engineering.

The primary functions of a lubricant are to:

- Reduce friction
- Prevent wear
- Protect the equipment from corrosion
- Control temperature (dissipate heat)
- Control contamination (carry contaminants to a filter or sump)
- Transmit power (hydraulics)
- Provide a fluid seal

Reducing friction may be a key objective of lubrication. However, there are several advantages to this method. Lubricating films will facilitate forestall corrosion by protective the surface from water and alternative corrosive substances. Additionally, they play a vital role in dominant contamination within systems.

1.3 LUBRICATION MECHANISMS

It is well known that the lubrication mechanism of the can is classified into:

1. Hydrodynamic Lubrication or Full Film Lubrication

Asperity contact is negligible in this case. The load is supported mainly by hydrodynamic pressure.

2. Mixed Lubrication

There is some asperity contact between the surfaces. The load is supported by both asperities and the liquid lubricant.

3. Boundary Lubrication

Solid surfaces come into direct contact. The load is supported mainly by surface asperities due to which there is high friction between the surfaces.

Fig. 1.4 below shows the above mentioned three types of lubrication phenomenon :

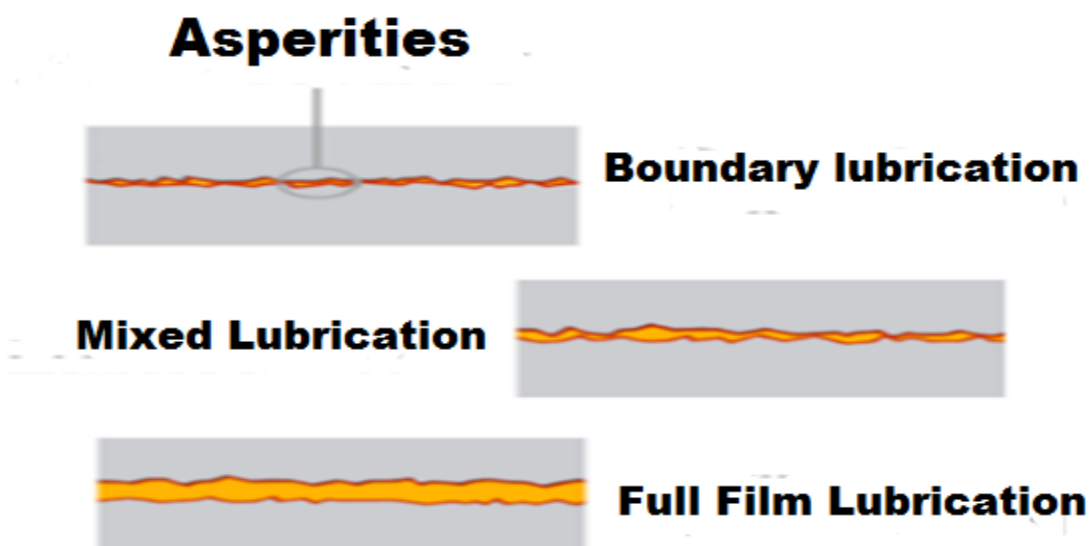


Fig 1.4: Types of Lubrication

1.4 STRIBECK CURVE

The Stribeck Curve is a fundamental concept in the field of tribology. It clearly shows the difference between lubrication mechanisms as the demarcation between full fluid-film lubrication and solid asperity interactions [8] as shown in Fig. 1.5.

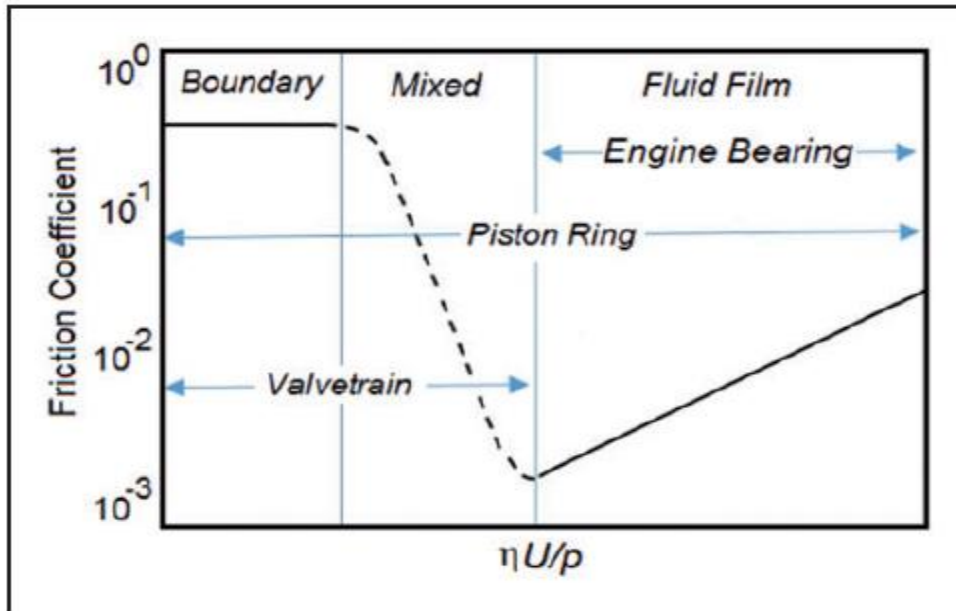


Fig. 1.5 Stribeck curve distinguishes lubrication regimes of engine components.

1.5 WEAR

Wear occurs between the two contacting surfaces whenever the lubricating film failure happens. This failure lessens the relative movement between the solid bodies and ultimately damages the contacting surfaces. There are different mechanisms through which wear occurs. These mechanisms are as follows:

- **Adhesive wear:** Adhesion wear is a result of micro-junctions caused by welding between the opposing asperities on the rubbing surfaces of the counter bodies. The load applied to the contacting asperities is so high that they deform and adhere to each other forming micro-joints.

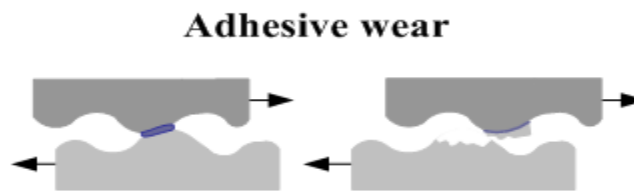


Fig 1.6: Adhesion Wear

- **Fatigue wear:** This wear is initiated by the fatigue processes due to the repetitive stresses under either sliding or rolling. Intervening films are effective then milder forms of wear. These milder form of wear are termed as fatigue wear. Fatigue wear of material is caused by a cycling loading during friction. Fatigue occurs if the applied load is higher than the fatigue strength of the material. Fatigue cracks start at the material surface and spread to the subsurface regions. The cracks may connect to each other resulting in separation and delamination of the material pieces.

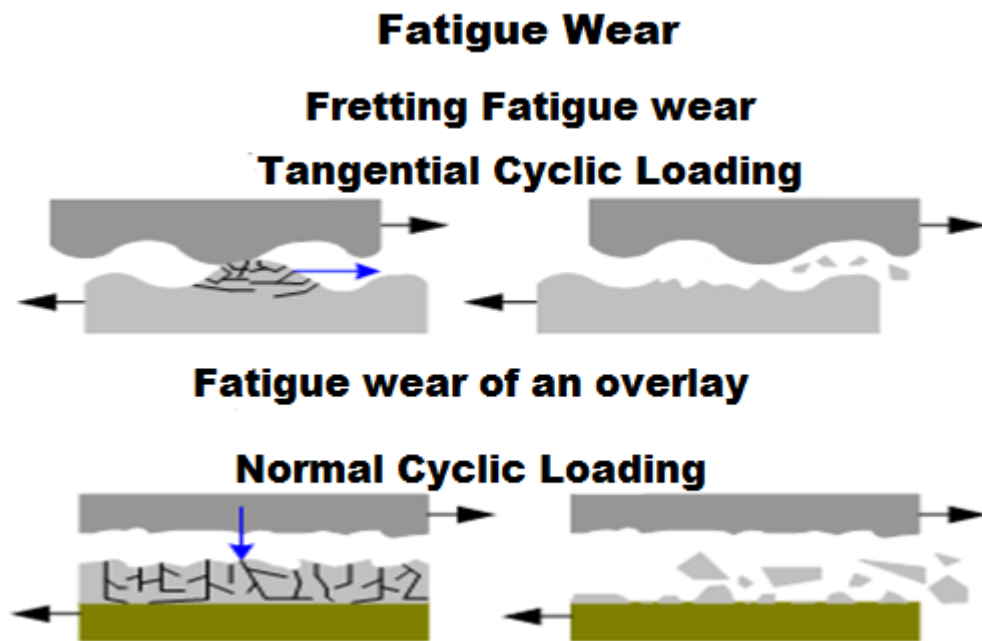


Fig 1.7: Fatigue Wear

- **Abrasive wear:** Sometimes the film material contains hard particles which flows over one body and causes wear to occur through ploughing action of the hard particles on the solid surface.

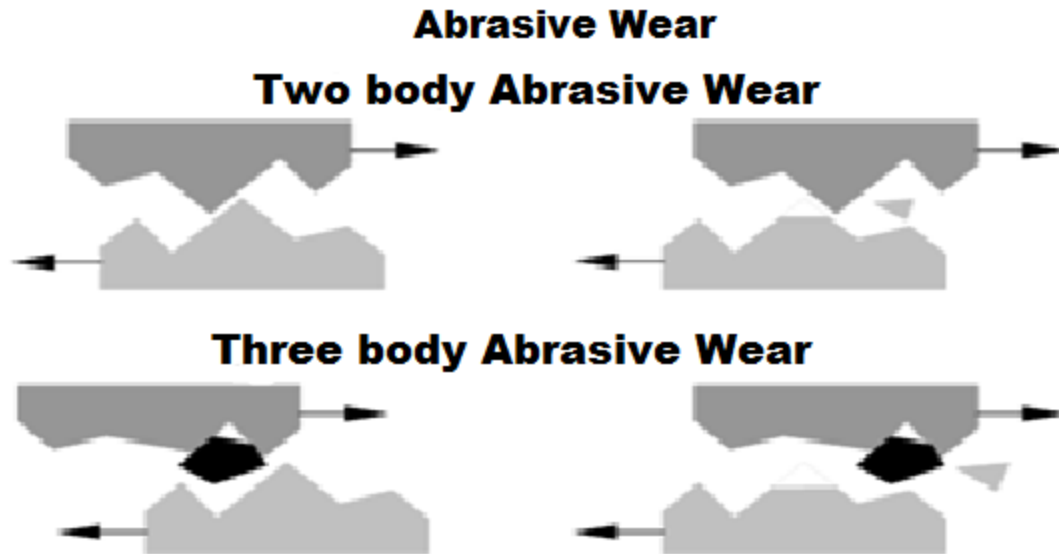


Fig 1.8: Abrasive Wear

- **Erosive wear:** It is caused by impingement of particles (solid, liquid or gaseous), which remove fragments of materials from the surface due to the momentum effect.

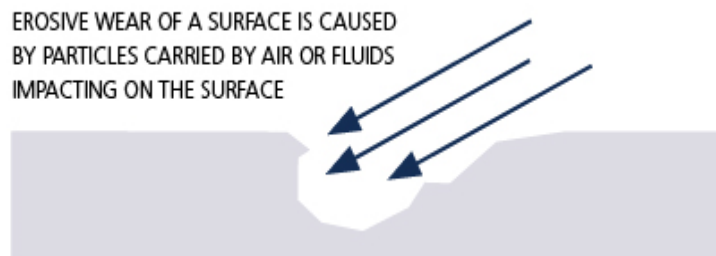


Fig 1.9: Erosive Wear

- **Corrosive wear:** Corrosive wear happens when material loss or degradation occurs due to chemical reactions with the part's surface and the surrounding environment. Environments include humidity, salt water, caustic solutions, acid, etc.

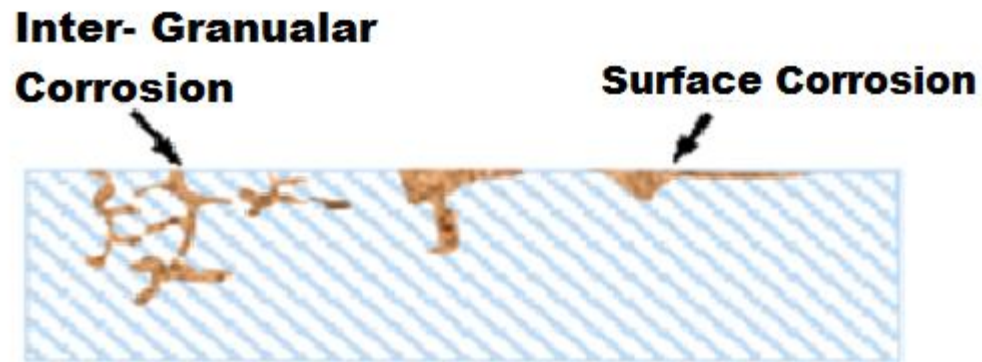


Fig 1.10: Corrosive Wear

1.6 PISTON RING AND CYLINDER LINER

1.6.1 PISTON

A piston, which is cylindrical engine component, this cylindrical engine part slides back and forth within the cylinder bore by forces produced throughout the combustion technique. The piston works as a movable end of the combustion chamber. The stationary part of the combustion chamber is the head of the cylinder. Pistons are a unit normally fabricated from an aluminum alloy for good and light-weight thermal conduction.

Piston features embody the piston pin, piston head, ring grooves, piston pin bore, skirt, ring lands, and piston rings.

A ring groove could be a recessed space situated round the perimeter of the piston that's accustomed retain a piston ring. Ring lands area unit the two parallel surfaces of the ring groove that perform because of the protection surface for the piston ring. A piston ring n is associate degree expandable split ring accustomed offer a piston ring between the piston associate degree the cylinder wall. Piston rings area unit normally made up of forged iron. Forged iron retains the integrity of its original form underneath heat, load, and different dynamic forces. Piston rings also seal combustion chamber, conduct heat from Piston to the cylinder wall, and come back oil to the housing. Piston ring size and configuration vary looking at engine style and cylinder.

1.6.2 PISTON RINGS CLASSIFICATION

Piston rings are comprised of compression rings, located towards the top of the piston and oil-control (scraper) rings, located below the compression rings.

In internal combustion engines, there are total of 3 rings are used

1. Two compression rings and
2. One oil scrapper ring.

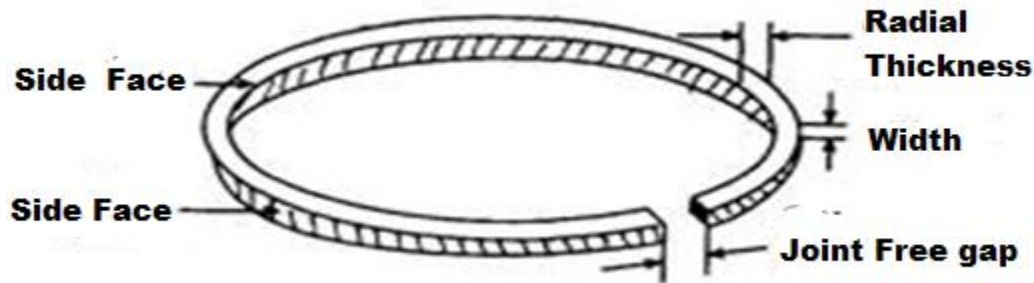


Fig. 1.11 Piston Ring

ROLE OF COMPRESSION RINGS

The compression ring acts as a gas seal between the piston and the liner wall, preventing the combustion gases' passage from the combustion chamber to the crankcase.

Compression rings prevent the motion of excessive pressure combustion products from the piston crown facet to the crankshaft facet.

The ring force distribution depends on the face form. With a rectangular face profile, the force is higher than with a barrel-shaped face, as the compression pressure can act on the face-side of the barrel-shaped ring against the ring pre-tension action. Plain compression rings, with a rectangular cross section, meet satisfactorily the sealing demands of ordinary running conditions and this type of compression ring is the most common one.

Role of Oil Scrapper Rings

Oil scrapper rings hold the uniform thickness of the lubricating oil between the cylinder liner and the piston rings. Whenever there is excess or deficiency of the lubricating oil, the oil scrapper ring satisfies the corresponding want of the oil. In other words, the oil rings control the flow of oil along the cylinder walls and keep oil from getting into the combustion chamber.

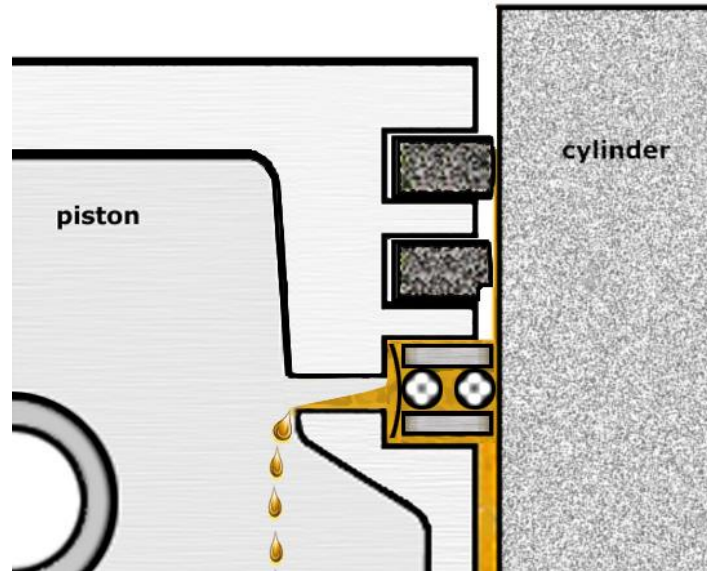


Fig 1.12: Compression Rings and Oil Scrapper Rings

1.6.3 CYLINDER LINER

Cylinder liner is a part of the cylinder block. It is only a cylinder with a small thickness. It made interference match with the cylinder block. It is one of the crucial surfaces of the engine. It is the surface on which the sliding of the piston ring happens. It keeps the lubricating oil among the cylinder liner and the piston ring. A cylinder liner should have the large anti-galling characteristics, high wear resistance, also have to cause less wear to the counter contacting surface i.e., piston ring surface. The liner also receives the heat from the combustion chamber via piston and piston ring and pass on this warmness to the coolant. Therefore the material used for the cylinder liner must have the excessive the thermal conductivity.

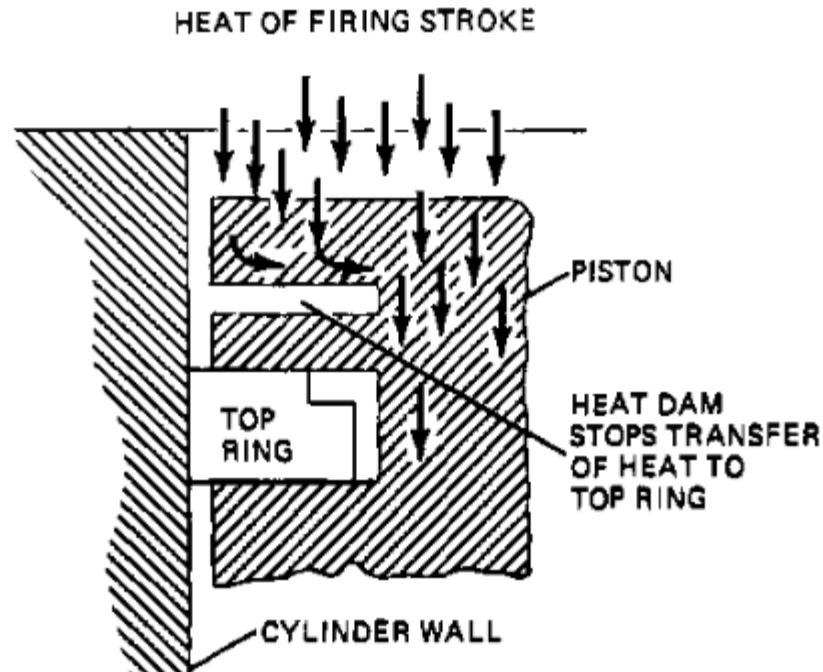


Fig 1.13: Heat transfer in the piston ring and liner assembly.

The cylinder liner needs to have the high-quality surface finish. It additionally prevents the excessive pressure and temperature fuel from leaking out to outside. The cylinder liner material must be hard so that it can't be transformed without difficulty under the have an impact on of high pressure and high temperature.

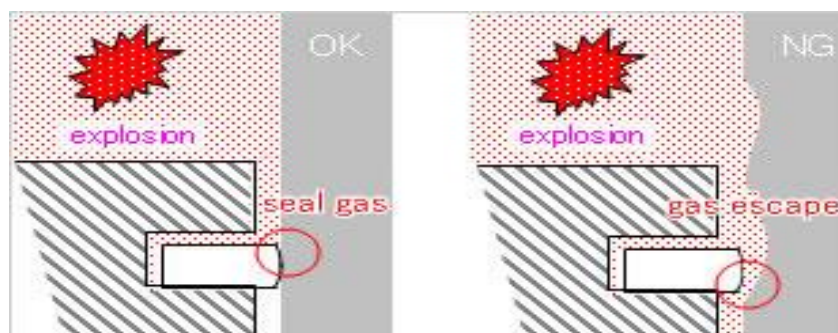


Fig 1.14: Leak proof Cylinder liner.

Cast iron is the generally used material for the cylinder liner as it offers good to wear on resistance properties. Steel is also used for the liner material as it has high stiffness and Strength.

These two are essential for the liner. Wear price is reduced after the use of the steel as the liner material. For this research work, mild metallic is used as a testing material similar to the liner.

Blow By in Internal Combustion engines.

Blow by is the situation in which the high pressure and high temperature gases from the combustion chamber side leak out on the crank case aspect. This condition occurs while the gap between the piston ring and the cylinder liner increases. An growth inside the gap between these surfaces is the end result of wearing out of the material. This leak out of the gases causes loss of the energy which in any other case can be applied in the turbocharger. So this makes the blow by a problem a critical issue which needs to be resolved even as designing the piston ring and cylinder liner assembly. By converting the approach of lubrication, materials used for those components, use of a coating or nano debris are proved to be effective methods to resolve this problem.

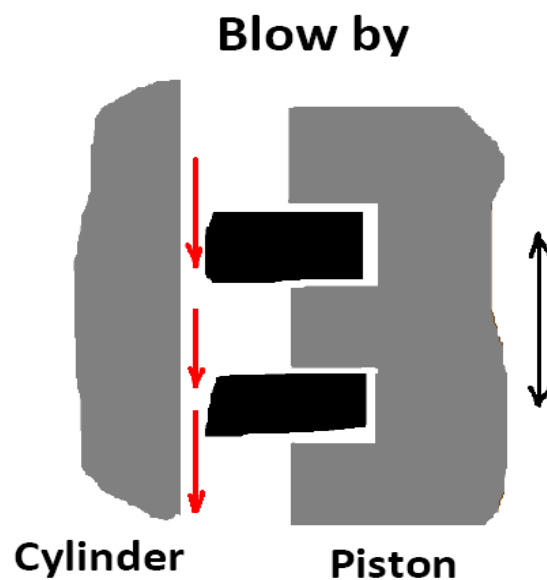


Fig 1.15: Blow By problem in IC engine.

CHAPTER 2: LITERATURE REVIEW

The first evidence of hydrodynamic lubrication between a piston ring and cylinder wall was reported by Hawkes and Hardy in 1936. Their friction measurements indicated that hydrodynamic lubrication prevailed throughout most of the engine cycle, the application of hydrodynamic lubrication theory to piston-ring analysis was pioneered by Castleman. Almost 20 years later, Eilon and Saunders conducted another lubrication analysis of a piston ring and reported the oil-film thickness and the friction force. These early studies applied a simplified hydrodynamic lubrication theory to this problem and neglected the squeeze film effect. Later, a higher degree of sophistication was achieved in theoretical studies of ring lubrication by Furuham, Lloyd, Baker, et al. Hamilton and Moore and others. Equally important experimental studies were also reported to support the theoretical investigations of this problem. Furuham, for instance, reported good agreement between theory and experiment at the mid-stroke position.

(Ting et al., 1974)[3] have developed theory including the considerations of the hydrodynamic lubrication between the rings and the cylinder liner, piston ring geometric and elastic characteristics, gas blow-by through the ring pack, minimum film thickness permitting film lubrication, piston side thrust load and Archard's wear relation. The ring face profiles for four engines with various mileages have been measured and were found to be offset parabola. A general off centered parabola is used to represent the profile of the ring running surface. It was assumed that there is no pressure change in the divergent portion of the ring wedge in both strokes. It could be concluded that a highly curved ring has a very large film thickness at the center of the stroke, where the wedge action is predominant. The film thickness falls very rapidly at the ends of the stroke where the action changes to the squeeze film type. The flattest ring never achieves a large film thickness, even at mid-stroke, but the fall at the ends of the stroke is less severe. Hence, there must be an optimum ring shape profile existing between the highly curved and flat ring face which will give the greatest film thickness at the critical points near the top and bottom dead centers.

Jeng et al., 1978)[4] have derived a system of three equations to describe the starved lubrication condition. The system takes the amount of lubricant supplied as an input and treats the lubricant inlet position as an unknown. The lubricant inlet position can be obtained directly by solving the system of equations. Thus, a direct approach is provided to conduct the starved lubrication analysis with a given lubricant supply. To determine the lubricant availability for the starved lubrication analysis a postulate for the lubricant transport phenomena in a complete ring pack is proposed. This postulate considers the flow continuity, oil accumulation and the relative location of the rings in a ring pack. In some instances, especially when squeeze motion dominates, there would be no cavitation. The exit boundary condition will then be $p(b/2, t) = P_T$ where p is hydrodynamic pressure at a point along the width of the piston ring; b is the width of the piston ring, and P_T is Pressure on the trailing edge. It is shown that boundary lubrication as indicated by film thickness ($\sigma_{comp.} = 0.37 \mu\text{m}$) occurs in the vicinity of either top or bottom dead center due to very small sliding velocity. This qualitatively agrees with the wear pattern observed on cylinder liners which show higher wear at the top and bottom of the stroke. Effect of engine speed, ring tension, ring width, crown height and offset on power consumption has been presented.

(Wakuri et al., 1979)[5] have assumed that the oil-film pressure at the oil inlet is equal to the ambient pressure, and the oil film breaks down on the downstream side according to the Reynolds boundary condition. After the oil film breaks down, the oil is carried into a cavitated region. The pressure in the cavitated region is constant with respect to the ambient pressure. When the piston rings were used as a ring pack, the oil supplied to each ring is dependent on the amount of oil left on the liner by the preceding ring. The subsequent rings presumably operate in a starved condition where the inlet region of a ring is incompletely filled with oil even if the leading ring is fully flooded with oil. Therefore, the analysis that the oil is copiously supplied to the rings at all times does not seem reasonable. The interaction between the rings in a ring pack is determined by the condition of oil-flow continuity if the oil is neither supplied nor extracted between the rings.

(Miltios et. al, 1989)[7] have assumed that the ring have a circular profile in the direction of motion and assumed the bore to be elliptic. Tilting of the ring is also taken into account. When the oil film is thick enough so that there is no surface to surface contact of the slider and the plane, the lubrication is hydrodynamic. When the oil film is not thick enough there is surface to surface contact (contact of the asperities of the two surfaces) and the lubrication is mixed because part of the load is carried by the oil film and part of it by asperities. The oil film thickness beyond which hydrodynamic lubrication exists cannot be determined accurately. It depends upon the topography of the surfaces and height of the asperities.

(Akalin et.al, 1999)[9] have investigated the effects of running speed, normal load, contact temperature and surface roughness both experimentally and numerically for conventional cast-iron cylinder bores. The author has shown the effect of two contact temperatures: 24°C and 70°C on the oil film thickness. Higher temperatures lead to lower viscosity. Therefore, lubricant film thickness and load carrying capacity of the oil film decrease significantly with increasing temperature. Mixed lubrication occurs throughout the stroke at the higher temperature 70°C and the tendency to cavitate increases over most of the stroke. The effect of the elliptical cylinder liner and friction heat on the piston ring pack was taken into account in the lubrication analysis of the gasoline engine. The result shows that the elastic deformation significantly affects the tribological performance of piston ring.

(Bolander et al, 2001)[10] have used twin fiber optic displacement sensors to accurately measure the lubricant film thickness experimentally. The analytical model developed by them can capture the different lubrication regimes that the piston ring and liner experience. They developed a model to investigate the lubrication condition between a piston ring and cylinder liner. It was assumed that the contact operates under fully flooded conditions except at the top and bottom dead centers and the mode of cavitation is closed form. A significant amount of surface interaction may occur near TDC and BDC where hydrodynamic action is at a minimum. In these mixed lubrication regions the applied load will be balanced by contributions from both the fluid pressure and the surface asperities in contact.

(George et al, 2007)[12] have predicted and compared their results with results from other semi-empirical models. In early studies, the squeeze film effect was neglected and a simplified hydrodynamic lubrication theory was applied to predict the oil film thickness. The model proposed by the authors considers that the complete ring pack can be reduced to a set of several compression rings and one twin-rail oil control ring. Each rail of the oil control ring is manipulated as a separate single ring. For the simulation of the oil film action between the piston ring and the cylinder liner, the one-dimensional Reynolds equation is used, considering sliding and squeeze ring motion.

(Abu-Nada et. al, 2008)[13] have approximated the shape of the oil film thickness by a trigonometric function where oil film thickness has minimum values at BDC and TDC and higher values in between. In the current study, the authors have assumed following distribution: $h(\theta) = A + B \sin(\theta)$ where, A and B are constants. h_m is the oil film thickness between the ring and cylinder liner. This thickness reaches a minimum value at the bottom dead center (BDC) and top dead center (TDC) and has higher values between them. Increasing the number or thickness of piston rings increases piston friction and thus reduces the brake power and the efficiency. However, the effect of changing piston ring configuration is limited in comparison to other parameters. This is due to dominance of skirt friction over ring friction. The author examined the effect of speed and temperature on efficiency for three different oil film distributions. Although decreasing oil film thickness results in a drop in efficiency, this effect becomes noticeable only at low temperatures and at high engine speeds. It is also interesting to note that the two distributions assume maximum film thicknesses of 7 μm and 12 μm resulted in nearly identical efficiency curves. However, the distribution that assumes a maximum film thickness of 2.5 μm resulted in a somewhat different curve. This suggests that there exists a threshold value in the order of 1 μm for the oil film thickness, below which ring friction can start to play significant role in piston friction.

(Gulwadi et.al, 2008)[14] have considered reattachment of the oil film with the ring due to the Jakobsson-Floberg Olsson (JFO) boundary condition after the film detachment. Over an engine cycle the scraping of rings against the liner causes oil to accumulate at the leading and trailing edges of each ring. During the flow of gases through the land/groove regions, a fraction of this lubricant is transported by these gases toward the combustion chamber during blow-back. Additionally, a fraction of the oil accumulation above the top ring is discharged toward the combustion chamber by throw-off due to inertia. The study conducted by the author involves the implementation of a mass-conserving (cavitation) scheme in the solution of the one-dimensional hydrodynamic lubrication equation for the piston ring. This scheme, in conjunction with a boundary lubrication model and oil transport model, facilitates the computation of the volume accumulation of oil for the ring at its leading and trailing edges. The trailing height of the oil film behind the ring is also computed, which is used in the estimation of the axial oil film distribution on the liner at each instant. From this information the amount of oil available for lubricating the ring at each instant of the cycle can be calculated.

(D V Bhatt et.al, 2009)[15] have investigated major factors affecting the oil film thickness are, piston speed, lubricant viscosity, ring face profile, boundary conditions, surface roughness, effect of ring twist, bore distortion and ring flexibility. Models are developed either on the assumption of Reynold's theory of hydrodynamic lubrication or Stribeck curves, the same are established for rotary motion while in PRA system the motion is reciprocating, so results may not have the consistency. A need to develop versatile model for reciprocating motion of piston assembly exists as lubrication regimes varies from Boundary to Hydrodynamic. Film thickness may vary from about 2.5 to 8 micron in power stroke with SAE 10W50a oil at 1600 rpm & no load conditions as predicted by Harigaya et al. It was assumed that there is no pressure change in the divergent portion of the ring wedge in both strokes. It could be concluded that a highly curved ring has a very large film thickness at the center of the stroke, where the wedge action is predominant. The film thickness falls very rapidly at the ends of the stroke where the action changes to the squeeze film type. The flattest ring never achieves a large film thickness, even at mid-stroke, but the fall at the ends of the stroke is less severe. Hence, there must be an optimum

ring shape profile existing between the highly curved and flat ring face which will give the greatest film thickness at the critical points near the top and bottom dead centers.

(S J Söchtig et.al, 2009)[16] have studied an experimental study of an investigation into the effect of load on the minimum oil film thickness between piston rings and cylinder liner in a fired compression ignition engine. Oil film thickness data were collected using capacitance-based transducers located near top dead centre and mid-stroke. Experiments were performed at 2000 r/min using two mono-grade oils (SAE 50 and SAE 20) and one multigrade oil (SAE 5W50) under a range of fixed engine loads. The experimental data obtained are discussed in the context of experimental and theoretical work published by other investigators.

(I Sherrington, 2011)[17] has studied about oil film thickness and on its development and use as a tool to study the hydrodynamic lubrication of piston rings in internal combustion engines. This includes the development of experimental sensors to measure lubricant film thickness and a review of phenomena related to the hydrodynamic lubrication of piston-ring packs. Computational model was prepared for the study of piston ring phenomenon and measuring the oil film thickness using the vital sensors at positions and the experimental data was compared with the computational method and error was commutated between the two methods.

(Avan et.al, 2012)[18] have investigated a reciprocating test rig combined with an ultrasonic film thickness measurement system was used for the tribological investigation of the piston ring-cylinder liner contact. Furthermore, a numerical model has been developed for all lubrication regimes to predict the film thickness and friction. A special piston ring and cylinder liner holder were designed and five sensors were glued on to the back side of the liner specimen. Ultrasonic reflections captured by the sensors, used to obtain the film thickness and friction were continuously recorded as the piston ring reciprocated over the liner. Several experiments have been performed at different speed and load conditions. The experimentally measured film thickness and friction are compared with the output from the numerical model and correlation

was found. Ultrasound proves an effective way of measuring film thickness, an invaluable aid for understanding the lubrication regime in a tribological contact and for validating simulations. Cavitation occurs in the contact which can adversely effect the ultrasonic measurement of film thickness, however this is detectable in the reflection coefficient profile and only affected the tests in one sliding direction.

(A. Sonthalia et. al,2013)[19] have studied about the friction between piston ring pack and cylinder accounts for major portion of friction in an internal combustion engine and it also significantly affects the mechanical efficiency of the engine. In the piston ring pack, friction is mainly due to the compression ring, especially at the top dead centre and bottom dead centre where boundary lubrication exists. A MATLAB code was generated for ring friction. Three different ring profiles were selected and analysed for lubricant film thickness, ring twist angle, ring friction and friction coefficient. Out of these three, friction force and friction coefficient of one ring profile design was found minimum. The ring design with minimum friction force and friction coefficient was manufactured and assembled in a low speed SI engine. The engine liner was modified to float and friction of the ring was studied using motoring test method. The experimental results were compared with the simulation result, it was found that simulation result was in agreement with the experimental result.

(Bedajangam et.al, 2013)[20] have investigated in IC engine piston ring friction losses account for approximately 20% of total mechanical losses as reported in the literature. A reduction in piston ring friction would therefore result in higher efficiency, lower fuel consumption and reduced emissions. To reduce these losses, various parametric approaches are made particularly at design stage and experimental level. The goal of this study was develop piston ring designs to improve engine efficiency, without adversely affecting oil consumption, blow by, wear and cost. Thus it provides characterization of a pressure balance in terms of effective area and distortion coefficient of the piston and cylinder. The models are for specific piston ring-liner system with different capacity. The variable parameters are piston velocity, engine speed, oil viscosity, gas pressure, crank angle film thickness and coefficient of friction. Non variable parameter are

system constant, bore diameter, ring tension, ring width, compression ratio, reciprocating mass, piston ring area and piston ring profile. The major assumptions for developing models are either hydrodynamic lubrication theory or mixed lubrication theory of Reynolds equation.

(Renlian ma et.al, 2015)[21] have studied the effect of surface texturing in the form of circumferential oil grooves on improving the tribological properties of piston ring cylinder liner tribosystem. Tests were performed on a reciprocating test rig with actual piston rings and cylinder liner segments, and a numerical model has been developed. A comparison was made between the performance of the textured cylinder liners and un-textured cylinder liners. It was found that with the smaller oil groove area density, the reduction in friction force is more obvious, Parabolic and triangular oil grooves are more efficient in friction reducing, and the prediction results by numerical model match the experimental results well in most case.

(Zhinan Zhang et. al, 2016)[23] have investigated to reduce the friction of a piston ring while maintaining a large oil film load-carrying capacity, an approach comprising of the inverse method and the sequential quadratic programming algorithm was proposed. The approach considers the variation of mixed lubrication and variable lubricant viscosity with temperature along the engine stroke, is developed to optimize the profile of a piston ring. A piston ring profile is represented by a polynomial function. A case study of the second piston ring shows that the proposed method can be applied for the optimization of a piston ring profile. In addition, this paper illustrates the effects of the degree of a polynomial function. The results show that the minimization of friction and maximization of oil film load-carrying capacity can be balanced simultaneously when the degree of the polynomial is 2 and 5.

(Garcia-Atance fatjo et.al, 2017)[24] have investigated the piston ring lubrication by comparing accurately calibrated experimental measurements of piston-ring film thickness in a firing engine with predictions from an advanced, commercial software package alongside details of the systematic analysis of the measurement errors in this process. Suggestions on how

measurement accuracy could be further improved are also given. Measurements of oil film thickness with an error (standard deviation) of +/-15% have been achieved. It is shown that this error can be reduced further, by changes in the design and installation of the sensors. Detailed experimental measurements of film thickness under the top compression ring in a firing petrol engine have been made and compared with the predictions from a commercial, state-of-the-art modelling package. The agreement between theory and experiment is excellent throughout the stroke in most cases, but some significant differences are observed at the lower load conditions. These differences are as yet unexplained, but may be due to the sensor topography influencing the hydrodynamic lubrication, lubricant availability, out-of-roundness in the cylinder, or squeeze effects.

(Cristiana Delprete et.al, 2017)[25] have studied reviews completely different models for evaluating piston ring-pack and liner lubrication, and frictional losses. The literature review indicates that piston ring– liner interface lubrication could be a complicated development, that incorporates a important impact on oil consumption and frictional losses. Analytical and numerical strategies for examining piston ring–liner trajectory losses and lubrication have received widespread attention from researchers due to the fact that piston ring-pack shows completely different behaviors in several things. Piston ring lubrication mechanisms have to be compelled to be totally understood to regulate oil consumption, frictional losses, and engine durability, that makes it necessary to conduct a comprehensive analysis. The synthesis of technical contributions for analyzing piston ring lubrication shows that small thought is given on the result of ring dynamics, lifting, and tilting, that incorporates a profound result on ring profile alterations and is directly joined to minimum oil film thickness and frictional losses. Finally, it's been found that Analytical modeling of piston ring–liner can be considered as AN applicable tool to assess the tribological performance of an engine.

CONCLUSIONS

It has been observed that the loss of fuel and power in the IC engine was a major issues and tribo pairs such as piston ring and cylinder liner plays a vital role for the fuel consumption and loss of power due to friction. The lubrication around the piston ring and liner thus becomes an important

parameter to study and analyze. Earlier researches deal with the hydrodynamic lubrication of piston rings and a parabolic profile was assumed for the piston ring to determine and simulate the pressure distribution, minimum oil film thickness and frictional force produced by the assumed profile. Firstly it was assumed that common forces acts on piston rings such as pressure force, tension force, the tilting effect on the piston ring was observed and the bending force also acts on the piston ring which effects its overall performance. That conclude that if ring profile is not uniform it can rotate about the piston which act dynamic in nature. Higher loads on piston caused fluid film thickness to be lesser. Various other effects such as change of oil viscosity with temperature and due to this the variation in performance of piston ring were affected. Study required to analyze the effect of the roughness and finishing of piston ring and cylinder liner and also its behavior on lubricant, load distribution with different zones of lubrication. The design optimization of piston ring profile was found to play important role to reduce the blow by and losses that can make the process more efficient.

Several work was available on lubrication action on piston ring and cylinder ring with hydrodynamic or mixed lubrication along with a parabolic profile of the piston ring and solved for pressure distribution, film thickness and frictional force. But no worn out case of piston ring was assumed which changed the profile of piston ring from initial parabolic. There is need to study a worn out piston ring profile and to generate polynomial profile using the curve fitting technique and other technique. The hydrodynamic lubrication in 2D phenomenon with pre assumptions modeling and simulating the profile for hydrodynamic lubrication at the ring profile and cylinder liner can be carried out. The fluid film thickness and pressure distribution with cavitation effect are required to be simulated.

CHAPTER 3: THEORETICAL MODEL

In this study, a model was developed to investigate the lubrication condition between a piston ring and cylinder liner. It is assumed that the contact operates under fully flooded conditions throughout the stroke. The following assumptions were made during the modeling:

1. Lubricant is Newtonian and incompressible;
2. The pressure is constant across the film.
3. Lubricant film thickness is circumferentially uniform;
4. Lubricant viscosity and density are constant.
5. Ring is fully engulfed and there is no cavity within the oil film thickness;
6. Thermal and elastic deformation of ring and liner are neglected;
7. The body forces and inertial effects are neglected.

3.1 FORCES ACTING ON PISTON RING

During the movement of piston along with the piston ring, various force acts on the piston ring due to the inertial effect, gas pressure across the piston ring, frictional force between piston rings and cylinder liner.

Piston rings are also subjected to tilting, the inner side of piston rings having a chamfered edge cause twisting (inner side of piston at tension) of the piston ring due to this the tip of piston ring gets tilted during the installation of piston ring with piston causing it to act as a cushion to stop the gas flowing through the piston ring and liner contact region. Therefore, twisting helps to reduce the blow by loss.

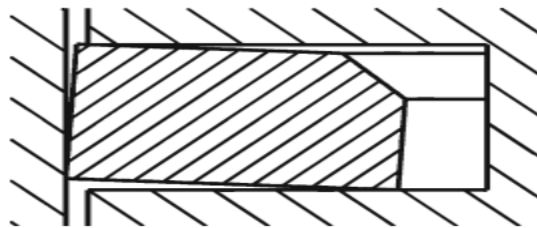


Fig. 3.1 Tilting in piston ring

There are two motions of a piston ring in IC engine:

- i) Axial movement
- ii) Radial movement

Below Fig. 3.2 shows the forces acting on the piston ring in both axial and radial direction.

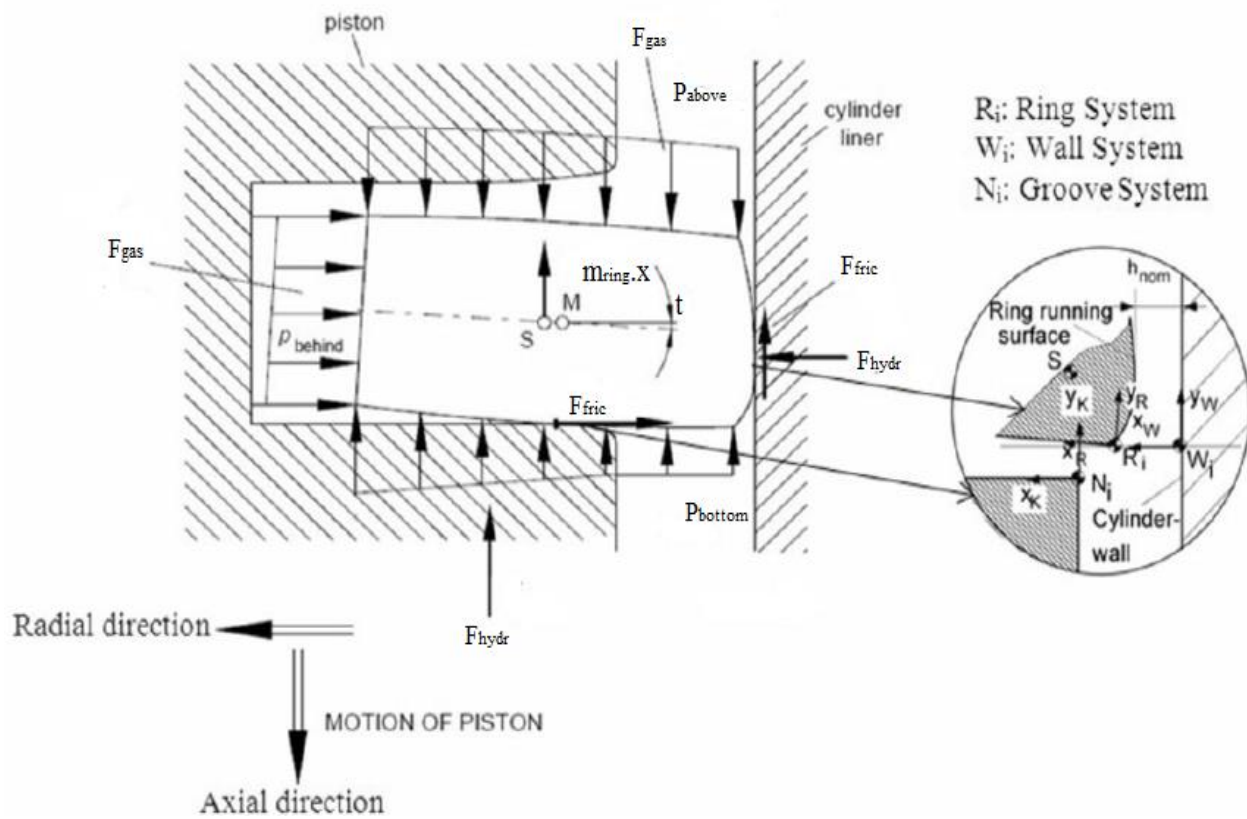


Fig. 3.2 Forces acting on piston ring

3.1.1 Forces on the piston ring during the axial movement

In the axial movement five different forces acts on the piston ring which are –

- a) Gas pressure force: It is due to the difference of pressure between above and below of the piston ring.
- b) Frictional force: It is due to the friction between cylinder liner and piston profile.
- c) Inertia force: It includes Gravity force and tilting force (due to change in velocity)
- d) Bending force: Due to interaction of thrust and anti-side thrust
- e) Damping force: Due to oil filling lubrication pressure development of the piston grooves.

$$F_{contact} = F_{gas} + F_{fric} + F_I + F_{bend} + F_{hydr}$$

$F_{contact} \geq 0$ Piston ring moves with piston, else it gets lifted from the groove.

Thus as piston is moving in Y direction, due to equilibrium.

$$m_{ring} * \ddot{Y} = F_{gas} + F_{fric} + F_I + F_{bend} + F_{hydr}$$

3.1.2 Forces on Piston Ring During Radial Movement

Similarly Forces across the radial direction can also be calculated using the equilibrium of forces across the radial direction

$$F_{contact} = F_{gas} + F_{fric} + F_{tension} + F_{hydr}$$

3.2 REYNOLD'S EQUATION

Reynolds equation is a partial differential equation governing the pressure distribution of thin viscous fluid films in lubrication theory. It has been used as governing equation to estimate the generated hydrodynamic pressure in piston ring/liner interface. [1]

When solving for the full ring the Reynolds equation needs to be expressed in 2D. With time dependence and the motion of the surfaces only in x-direction it can be written as:

$$\frac{\partial}{\partial x} \left(h^3 \frac{\partial p}{\partial x} \right) = 6 \eta U \frac{\partial h}{\partial x} + 12 \eta \frac{\partial h}{\partial t}$$

In the unused condition piston ring profile is straight/ rectangular but when under working condition the piston ring profile wears out, mostly at the middle mainly because of friction forces (acting as shear force) caused by lubricant oil flowing between the cylinder liner and the piston. There were many profiles which could be assumed for the worn out profiles like cubic, parabolic elliptical etc. But after observing a few of worn out rings, it can be noticed that worn out profile cannot be described by a single mathematical curve of two or three degree. So it can safely be assumed to use a combination of two curves and develop a single curve so as to develop the worn out profile.

To get mathematical model of the required profile, the profiles of parabola and ellipse are assumed to be merged as done further:

1). PARABOLIC PROFILE

To obtain the equation of parabolic profile, take the general equation of 2D curve i.e.

$$z = px^2 + qx + r \dots \dots \dots (1)$$

From the Fig. 3.3 given, the boundary conditions can be written as:

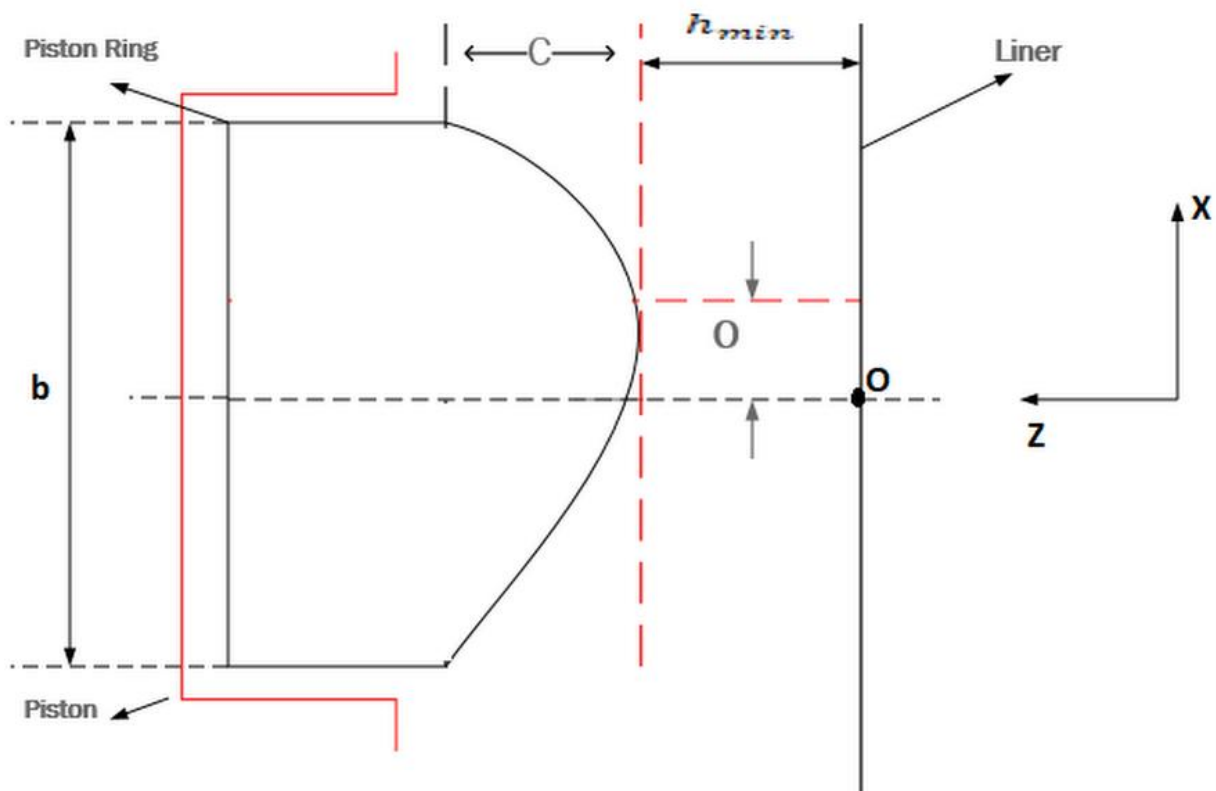


Fig 3.3: Model of Parabolically worn out piston ring face profile

$$1^{\text{st}} \text{ point} \rightarrow \left(-\frac{b}{2}, c+h_{min}\right)$$

$$2^{\text{nd}} \text{ point} \rightarrow \left(+\frac{b}{2}, c+h_{min}\right)$$

$$3^{\text{rd}} \text{ point} \rightarrow (0, h_{min})$$

Here, h_{min} represents the minimum oil film thickness between worn piston profile and cylinder liner. And, ‘o’ represents the offset distance of point where there is minimum oil film thickness from the origin so assumed. ‘b’ represents the overall width of piston ring over which fluid film is developed. ‘c’ is the distance between point of minimum oil film thickness to the end point of profile in lateral or z direction.

As equation of profile is assumed to be parabolic, it is generated by a 3-point parabola which are defined as above, to be put in equation 1 and obtain the constants in the equations in terms of parameters so considered.

After putting 1st, 2nd and 3rd point respectively in equation (1),

$$C+h_{min} = p \left(\frac{b^2}{4}\right) - q \left(\frac{b}{2}\right) + r \dots\dots\dots (2)$$

$$C+h_{min} = p \left(\frac{b^2}{4}\right) + q \left(\frac{b}{2}\right) + r \dots\dots\dots (3)$$

$$C+h_{min} = p(o^2) - q(o) + r \dots\dots\dots (4)$$

After solving equation 2nd, 3rd and 4th equation, constants obtained are:

$$P = \frac{c}{\frac{b^2}{4} - o^2} \dots\dots\dots (A)$$

$$q = 0 \dots\dots\dots (B)$$

$$r = h_{min} - \frac{c}{\frac{b^2}{4} - o^2} (o^2) \dots\dots (C)$$

Putting constants (A),(B) and (C) in equation (1), we get,

$$z = \left[\frac{c}{\left(\frac{b}{2}\right)^2 - o^2} (x^2 - o^2) \right] + h_{min}$$

assuming null ring offset for above equation, i.e., o=0, we get;

$$z = \frac{4c}{b^2} x^2 + h_{min} \dots\dots\dots (5)$$

The parabola so obtained from above equation is generated with the help of MATLAB. Code for the same is as shown below.


```

t=linspace(-2,2,100)           %span over which parabolic profile is considered%
x=t'
v=x.^2
c=1
b=4                             %total distance over which elliptical profile is assumed%
h=1*10^-3
g=size(v)
y1=max(g)
y1=zeros(y1,1)
y1=((4*c*v)/b^2)+h             %parabolic curve equation%
plot(x,y1)

```

The curve so generated in MATLAB is as follows:

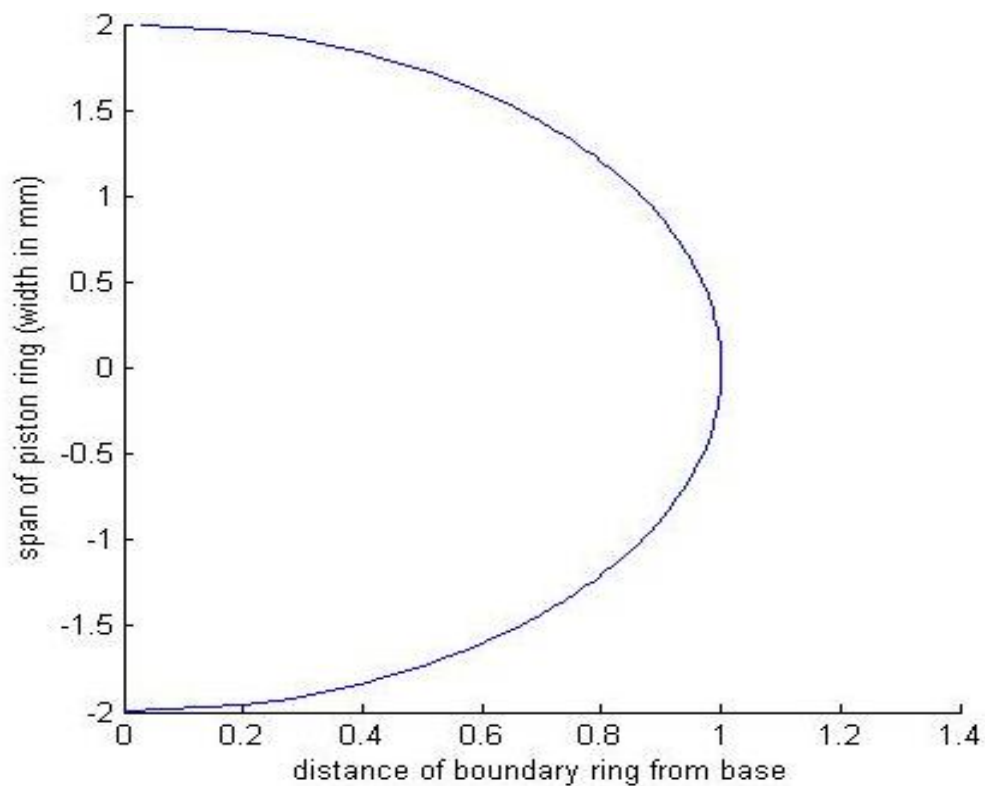


Fig. 3.4: Worn out piston ring face profile- Parabolic

2). ELLIPTICAL PROFILE

For an elliptical profile, general equation is of the form,

$$\frac{(x-a)^2}{p^2} + \frac{(z-b)^2}{q^2} = 1 \dots\dots\dots(6)$$

Where (a,b) are the corresponding elliptical centers and p, q are intercepts on x and z axes respectively.

Here centre of ellipse is at $(0, h_{min})$. Therefore, the above equation becomes;

$$\frac{x^2}{p^2} + \frac{(z-h_{min})^2}{q^2} = 1 \dots\dots\dots(7)$$

From the Fig. 3.5 the boundary conditions can be taken as :

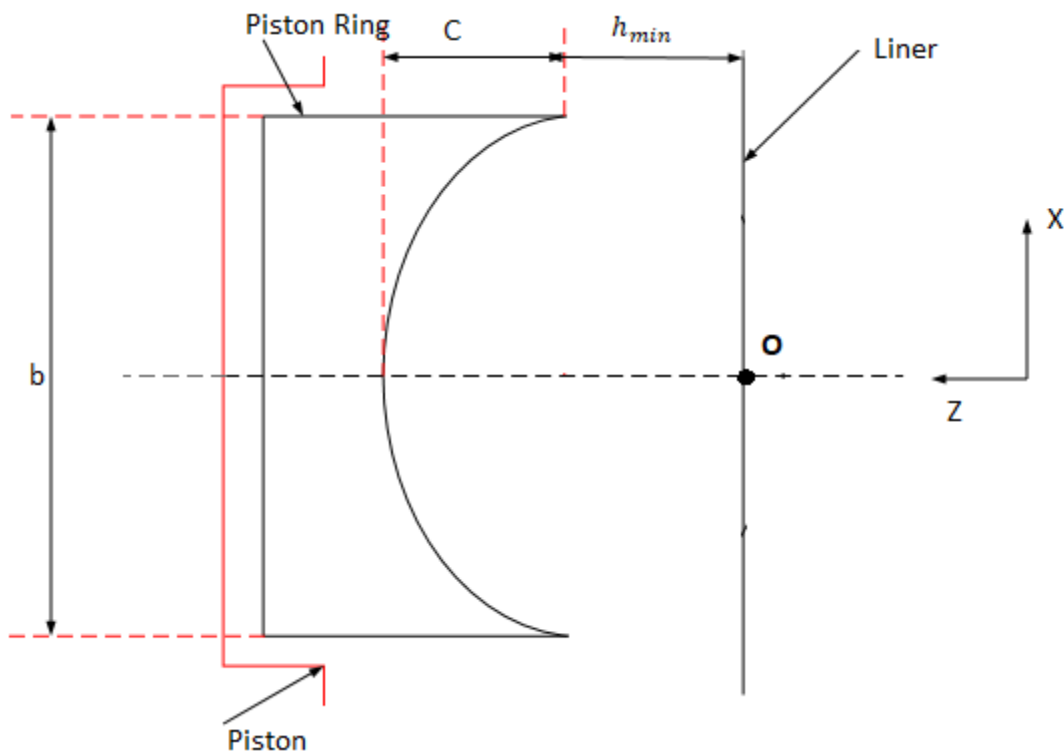


Fig 3.5: Model of Elliptically worn out piston ring face profile

1st point $\rightarrow (0, c+h_{min})$

2nd point $\rightarrow (\frac{b}{2}, h_{min})$

3rd point $\rightarrow (-\frac{b}{2}, h_{min})$

Here, h_{min} represents the minimum oil film thickness between worn piston profile and cylinder liner. And, 'o' represents the offset distance of point where there is minimum oil film thickness from the origin so assumed. 'b' represents the overall width of piston ring over which fluid film

is developed. 'c' is the distance between point of minimum oil film thickness to the end point of profile in lateral or z direction.

As equation of profile is assumed to be elliptical, it is generated by 3-point ellipses which are defined as above, to be put in equation 6 and obtain the constants in the equations in terms of parameters so considered.

Putting the above three boundary equations in the equation (7), we get constants p and q as,

$$q = \pm c$$

$$p = \pm \frac{b}{2}$$

Putting above obtained constants in equation (7), we get,

$$z = c \sqrt{1 - \frac{4x^2}{b^2}} + h_{min} \dots\dots\dots (8)$$

The ellipse so obtained from above equation is generated with the help of MATLAB. Code for the same is as shown below.

```
%%generate and plot elliptical profile%%

t=linspace(-2,2,100)    %span over which elliptical profile is considered%
x=t'
v=x.^2
c=1
b=4                    %total distance over which elliptical profile is assumed or width of piston ring%
h=1*10^-3              %minimum oil film thickness%
g=size(v)
y2=max(g)
y2=zeros(y2,1)
y2=(c*(sqrt((1-(4*v/(b^2)))))))+h %equation for elliptical profile%
plot(x,y2)
```

The curve so generated in MATLAB is as follows:

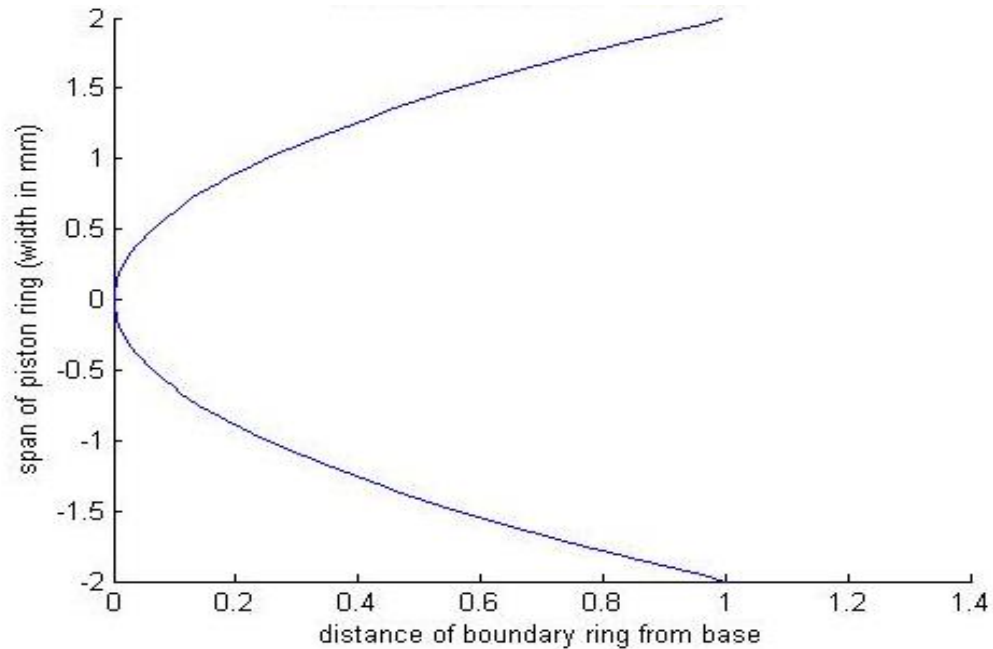


Fig: 3.6: Worn out piston ring face profile- Elliptical

There are some points worth noting about the consideration of piston ring profile which is needed to be modeled:

1. For pressure distribution in film that separates the mating surfaces, piston ring profile must have converging surfaces.
2. For middle portion should have cavity to trap the lubricant and debris and deliver when required.

Therefore, the need of most efficient piston ring face profile is there to be modelled. According to literature survey, it was observed that profiles at the end were near about parabolic and it was elliptical in the middle.

Thus, it is the combination of two profiles which is of prime concern here, so these two curves are plotted on a single plot. Then their intersection points are calculated and the outer ends are taken to be parabolic and the middle portion is taken to be elliptical.

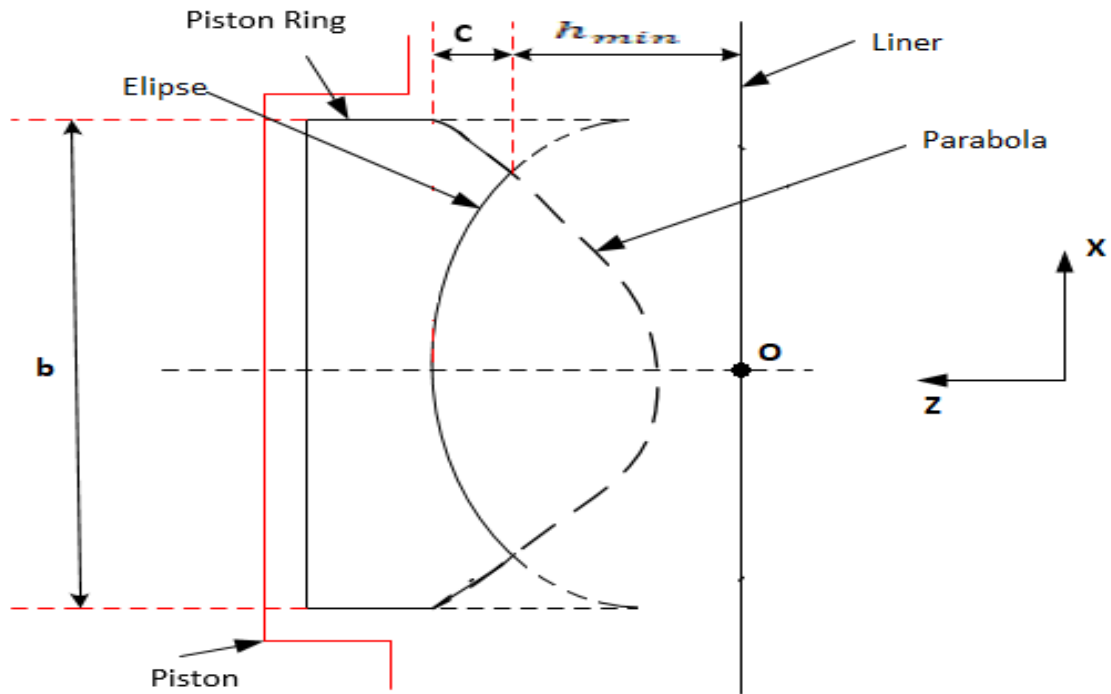


Fig. 3.7: Model of Parabolic and elliptical profile on same geometry.

Representation of above model in MATLAB is presented as follows:

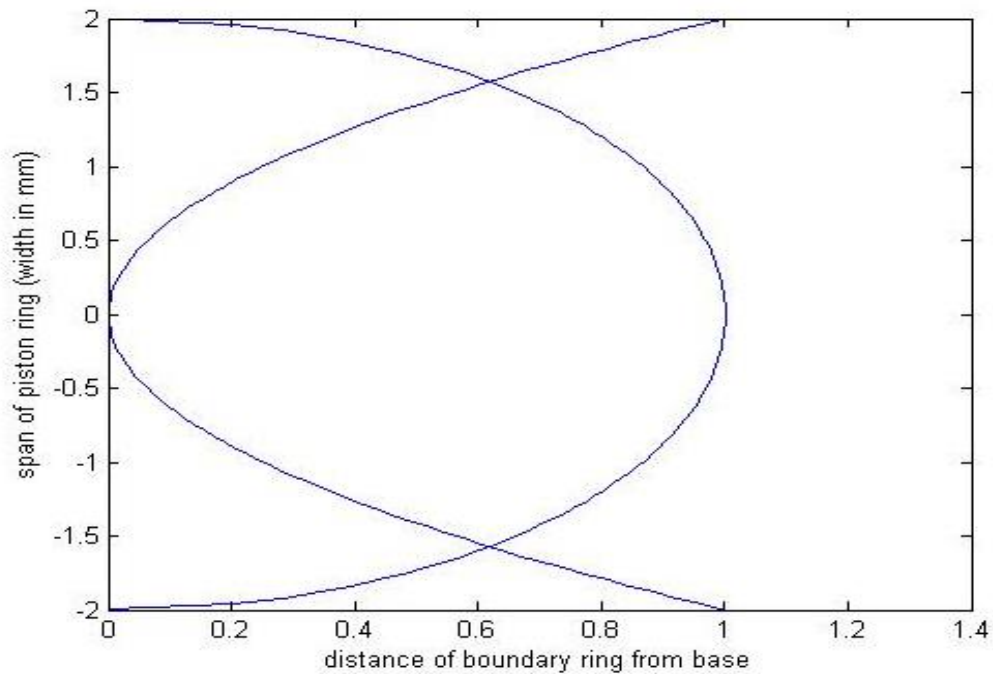


Fig. 3.8: Combining worn out piston ring face profile- Elliptical+Parabolic

The equations (5) & (6) of parabola and ellipse respectively are merged through MATLAB.Code for same is as shown below

```

%%obtain parabolic and elliptical profile on same graph%%

%parabolic profile%
t=linspace(-2,2,100)    %span over which parabolic profile is considered%
x=t'
v=x.^2
c=1
b=4                    %total distance over which elliptical profile is assumed%
h=1*10^-3             %minimum oil film thickness%
g=size(v)
y1=max(g)
y1=zeros(y1,1)
y1=((4*c*v)/b^2)+h    %parabolic curve equation%
plot(x,y1)

hold on

%elliptical profile%
t=linspace(-2,2,100)    %span over which elliptical profile is considered%
x=t'
v=x.^2
c=1
b=4                    %total distance over which elliptical profile is assumed%
h=1*10^-3             %minimum oil film thickness%
g=size(v)
y2=max(g)
y2=zeros(y2,1)
y2=(c*(sqrt((1-(4*v/(b^2)))))))+h %elliptical curve equation%
plot(x,y2)

hold off

```

Following equation represents the combined (parabolic and elliptical) profile of piston ring

$$Z \text{ (or) } h = 0.0682x^4 - 0.2951x^3 + 1.041 \dots\dots\dots(9)$$

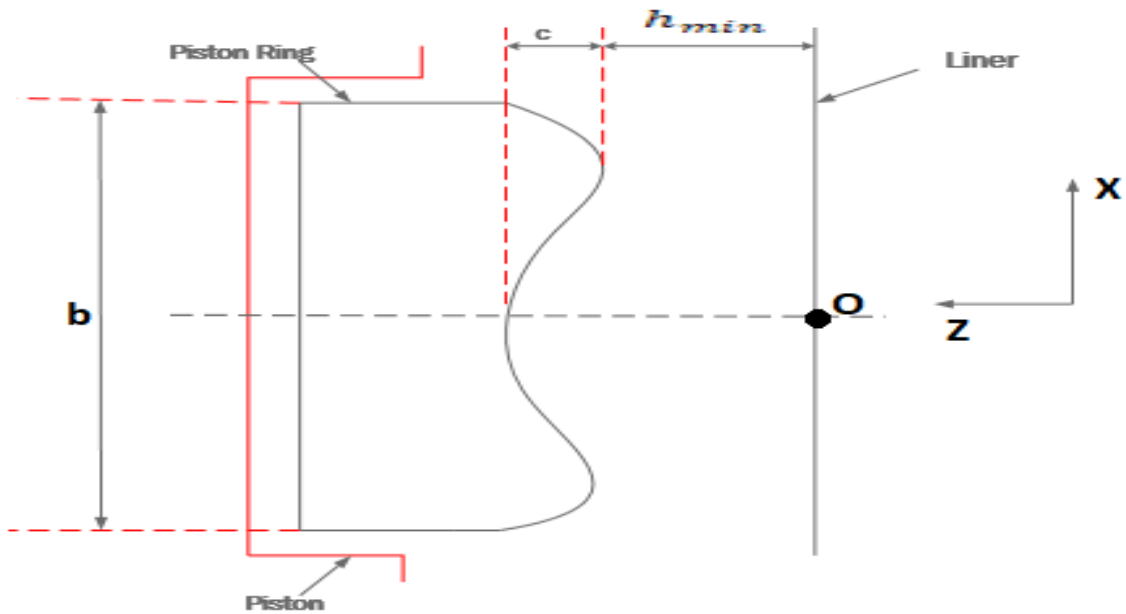


Fig. 3.9: model of piston ring combined face profile

Best curve fit for above equation 9) can be shown as with the help of MATLAB as below:

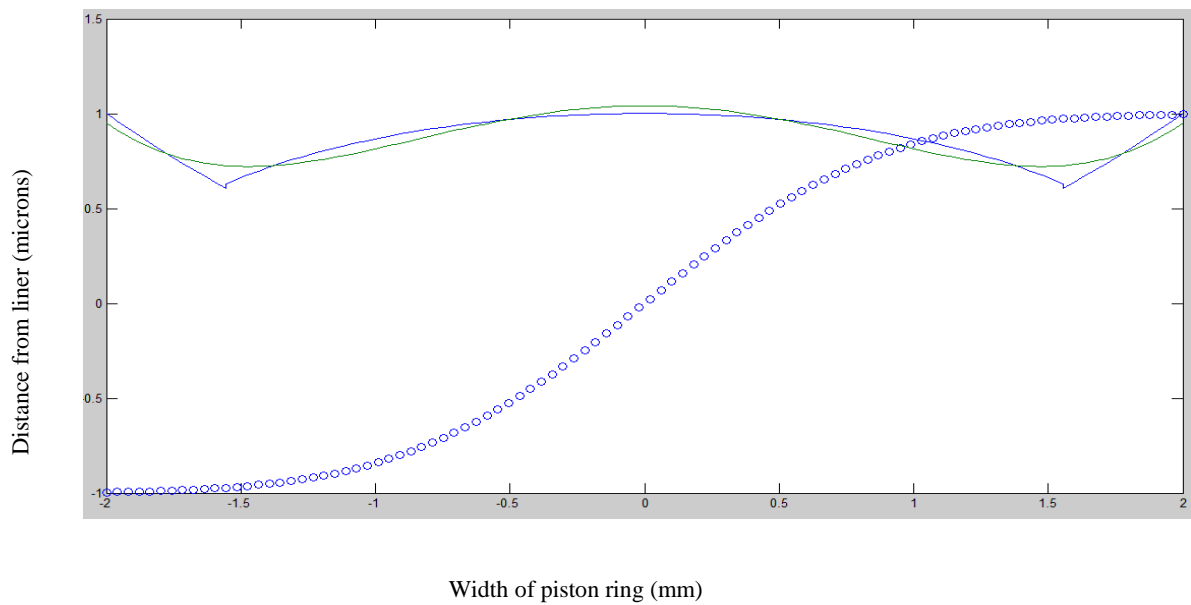


Fig. 3.10 Complete piston ring worn profile

The curve obtained is shown by the broken line, while the curve of best fit is shown in continuous.

Now, the displacement of piston in terms of crank angle θ , can be written as

$$x = r [(1 - \cos \theta) + (n - \sqrt{n^2 - \sin^2 \theta})] \dots \dots \dots 10)$$

It can be seen from the equation (10) displacement of piston is a strong function of $\cos(\theta)$, as we can safely assume that n (ratio of connecting rod to crank) is very large compared to maximum or minimum value of $\sin(\theta)$.

CHAPTER 4: RESULTS AND DISCUSSIONS

4.1 OIL FILM THICKNESS V/S CRANK ANGLE

The variation of fluid film thickness with the crank angle is obtained by replacing x in equation (9) by expression (10). The variation thus obtained is as shown in the graph below:

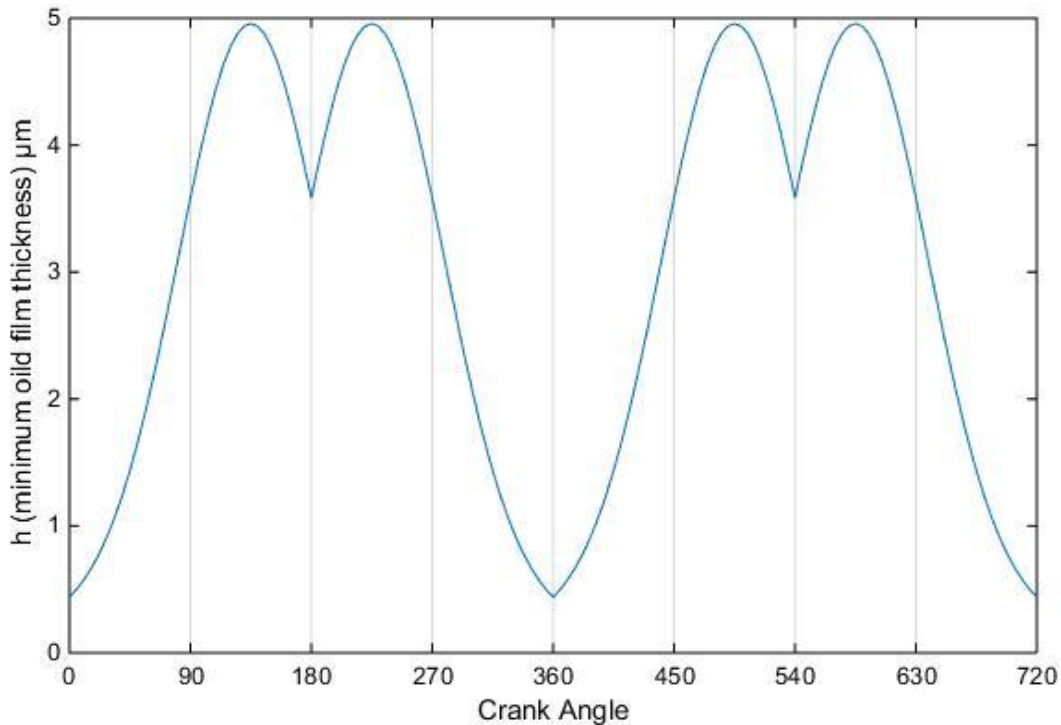


Figure 4.1: Predicted Cyclic Variation of Minimum Film Thickness

0-180 is suction stroke, 180-360 is compression stroke, 360-540 is power stroke and 540-720 is exhaust stroke.

Figure 4.1 shows the predicted cyclic variation of minimum lubricant film thickness with zero degrees of crank angle being TDC firing. The solution exhibits the expected characteristic shape of curve with small film thicknesses around the dead center positions where the entrainment velocity is small and large film thicknesses at the mid-stroke positions where the entrainment velocity is large. Film thicknesses on the power and exhaust strokes (0° to 360° crank angle) are generally smaller due to the higher gas loading on the rings and there is a step

change in both curves just after mid-stroke on the intake stroke (at approximately 470°) which is associated with a ring lift event when the ring moves from one side of the piston groove to the other with a consequent change in gas loading on the inner diameter of the ring.

4.2 PRESSURE V/S CRANK ANGLE DIAGRAM

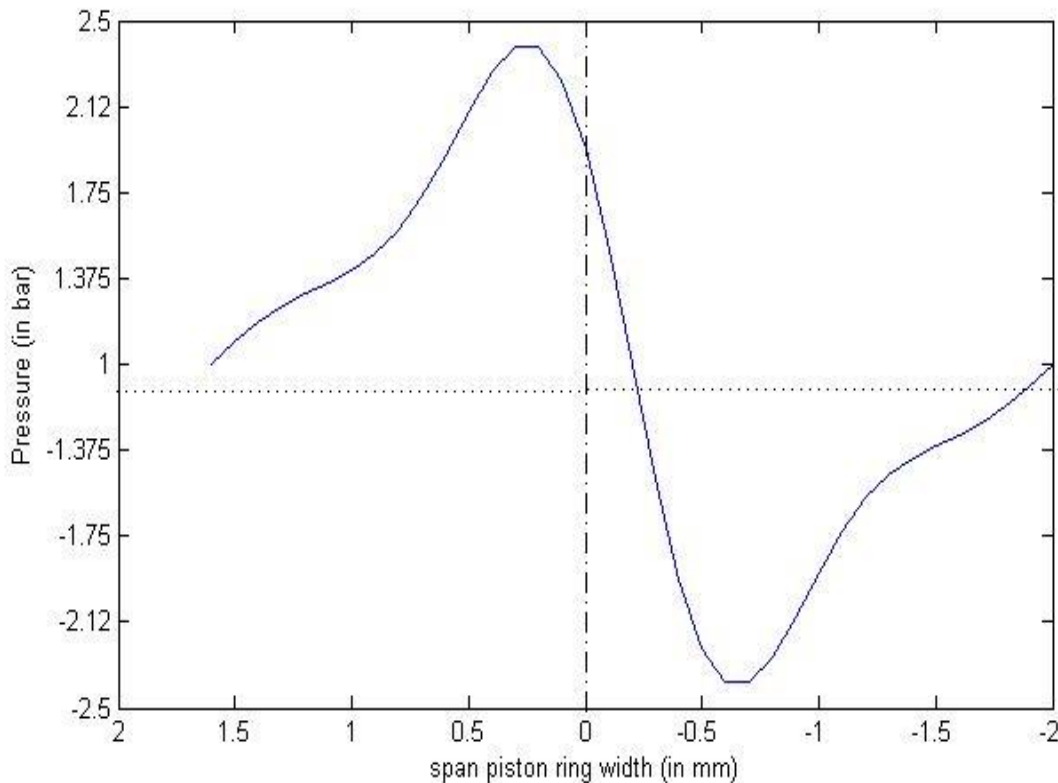


Fig 4.2: Variation of pressure v/s Width of piston ring

Flow separation takes place from the stationary surface when the cross-film velocity gradient is zero. In the piston ring / cylinder wall interface the piston ring is considered the stationary surface in terms of the hydrodynamic model and lubricant entrainment and thus the flow will separate from the piston ring at the outlet gas pressure subject to the pressure gradient condition. The hydrodynamic pressure profile is characterized most significantly by a small sub-ambient pressure loop upstream of the point of separation. In piston ring lubrication, gravity and inertia effects are negligible.

It is to be noticed that the negative pressure developed in the region, also known as cavitation region, is subjected boundary condition as there is possibility of rupture of oil film in the space between liner and piston ring but cavitation in the regime has very less chances of occurring. Minimum pressure in the hydro-dynamic layer is generally observed at the exit of piston ring.

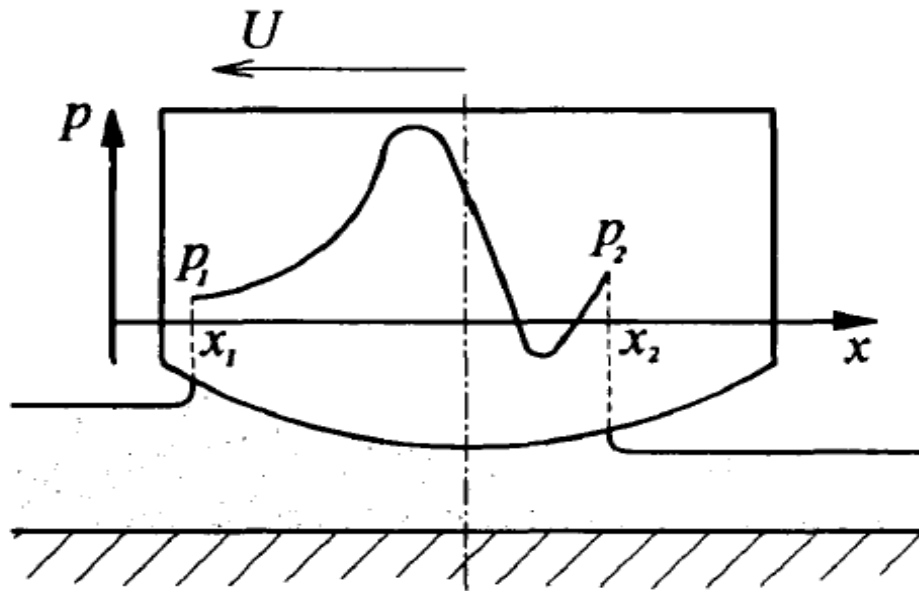


Fig 4.3: Variation of pressure with piston ring width – Reynold’s Condition (priest,1996)

It can be observed from figure 4.2 and figure 4.3 (priest,1996) that the trend of variation of hydro-dynamic pressure so obtained is in accordance with the trend predicted by in the literature. The trend obtained is based on simple Reynold’s equation (Appendix-1) which was the basic of development of fluid film thickness for modelled piston ring face profile. Thus it can be concluded our curve so generated is in compliance with the literature.

CHAPTER 5: CONCLUSIONS AND FUTURE ASPECT

5.1 CONCLUSIONS

It has been concluded that there is the potential to obtain different values of radial hydrodynamic force, and consequently to predict differences in lubricant film thickness, axial friction force and therefore frictional power loss. Also, the axial friction force F is influenced directly by the lubricant film thickness and also by the axial extent of the lubricant film. In all the conditions, the friction force in the regions with full fluid films is obtained by integrating the hydrodynamic and asperity contact shear stresses axially across the region.

The lubricant leaves the piston ring at the point of separation and there is no subsequent friction acting on the piston ring. Hence, the axial extent of the regions over which frictional shear stresses act very differently with cavitation and separation boundary conditions, leading to greater differences in total friction force and power loss than would be expected on the basis of film thickness variation alone. The required profile modelled by the observation of worn surfaces and modelled using MATLAB.

- 1) At both the ends parabolic face profile of piston ring has been generated.
- 2) Around the middle part of piston ring the elliptical profile was generated.
- 3) Finally, the combination of parabolic and elliptical profile was generated.

The best fit curve was obtained and fluid film thickness equation was found as follows:

$$Z \text{ (or) } h = 0.0682x^4 - 0.2951x^3 + 1.041$$

The variation of fluid film thickness with respect to the crank rotation has been plotted and found that small film thicknesses were developed around the dead center positions where the entrainment velocity is small and also the large film thicknesses at the mid-stroke positions were found where the entrainment velocity is large.

A curve for the variation of pressure distribution with respect to width of piston ring has been plotted and found that the flow will separate from the piston ring at the outlet gas pressure subject to the pressure gradient condition and minimum pressure in the hydro-dynamic layer was observed at the exit of piston ring.

5.2 FUTURE ASPECT:

- The model of piston ring face profile can further be verified with higher degree of curve which may generate better set of results.
- The pressure profile developed can be used to determine the friction force on the piston ring face. And thus, loss in power can be verified.
- A physical piston ring with such a profile can be made which can be analyzed to practically on an engine setup to validate for power losses.
- A change in lubricant properties can also be made.
- A better mechanism for debris collection can be developed as per the power loss in profile so obtained.

REFERENCES

- [1]. C. Hardy, Hawkes, "The Friction of Piston Rings," Trans. N.E. Coast Inst. Engrs. and Shipbuilder, vol. 52, pp 143, 1936
- [2]. R. A. Castleman, "A Hydrodynamic Theory of Piston Ring Lubrication", vol. 7, no. 9, pp.364-367, April 1939.
- [3]. J. E. Mayer, L. L. Ting, "Piston Ring Lubrication and Cylinder Bore Wear Analyses", Journal of Lubrication Technology, vol. 96, no. 2, pp. 258-266, April 1974.
- [4]. Y.R. Jeng, "Theoretical Analysis of Piston-Ring Lubrication Part I—Fully Flooded Lubrication", Tribology Transactions, vol. 35, no. 4, pp. 696-706, March 1978.
- [5]. M. Soejima, T. Taniguchi, Y. Wakuri, "Oil Film Behavior of Piston Ring", Trans. Japan. Soc. Mech. Eng., vol. 43, no. 370, pp. 295-302., 1979.
- [6]. C. Asahi, S. Furuhashi, M. Hiruma, "Measurement of Piston Ring Oil Film Thickness in an Operating Engine", ASLE Transactions, vol. 26, no. 3, pp. 325-332, Jan. 1983.
- [7]. G. K. Miltsios, D. J. Patterson, T. C. Papanastasiou, "Solution of the Lubrication Problem and Calculation of the Friction Force on the Piston Rings", Journal of Tribology, vol. 111, no. 4, pp. 635-641, Oct. 1989.
- [8]. A.W. Batchelor, G. Stachowiak, "Engineering tribology", in CA: Curtin University, 1993.
- [9]. A. Ozgen, G. M. Newaz, "Piston Ring-Cylinder Bore Friction Modeling in Mixed Lubrication Regime", Journal of Tribology, vol. 123, no. 1, pp. 211-218, Dec 1999.
- [10]. N.W. Bolander, B.D. Steenwyk, F. Sadeghi, and G. R. Gerber, "Lubrication regime transitions at the piston ring –cylinder liner interface", Journal of Engineering Tribology, vol. 219, no. 1, pp. 19-31, Jan 2001.
- [11]. G. H. Jiang, X.M. Chen, Ye, Y.C Zou, "Numerical investigation of the EHL performance and friction heat transfer in piston and cylinder liner system", in Proc. SAE World Congress, vol. 7, pp. 1-14, March 2004.

- [12]. G. A. Livanos, P.N. Kyrtatos, "Friction model of a marine diesel engine piston assembly", *Tribology International*, vol. 41, no. 10-12, pp. 1451-1453, Dec 2007.
- [13]. Abu-Nada, B. Akash, E. Al-Hinti, I. Al-Sarkhi, "Effect of Piston Friction on the Performance of SI Engine: A New Thermodynamic Approach" *ASME Journal of Eng. for Gas Turbines and Power*, vol. 130, pp. 022802-1 to 022802-8, 2008.
- [14]. S.D. Gulwadi, "Analysis of Tribological Performance of a Piston Ring Pack", *Tribology Transactions*, vol. 43, no. 2, pp. 151-162, March 2008.
- [15]. D V Bhatt, M A Bulsara and K N Mistry, " Prediction of Oil Film Thickness in Piston Ring - Cylinder Assembly in an I C Engine", in *Proc. World Congress on Engineering*, vol. 2, pp. 1-4, July 2009.
- [16]. I Sherrington, S J Söchting , "The effect of load and viscosity on the minimum operating oil film thickness of piston-rings in internal combustion engines", *Journal Engineering Tribology*, vol. 223, no. 3, pp. 383-391, Feb 2009.
- [17]. I Sherrington, " Oil film thickness measurement: a contribution to the understanding and control of lubrication in the piston-ring packs of IC engines", *Journal of engineering tribology*, vol. 225, no.7, pp. 595-601, June 2011.
- [18]. A. Almqvist , A. Spencer, E.Y. Avan, R.S.D. Joyce, R. Larsson, "Experimental and numerical investigations of oil film formation and friction in a piston ring–liner contact", vol. 227, no. 2, pp. 126-140, Nov. 2012.
- [19]. A. Sonthaliaa, C.R. Kumara, "The Effect of Compression Ring Profile on the Friction Force in an Internal Combustion Engine", *Tribology in Industry*, vol. 35, no. 1, pp. 74-83, April 2013.
- [20]. N. P. Jadhav, S.K. Bedajangam, "Friction Losses between Piston Ring-Liner Assembly of Internal Combustion Engine", *International Journal of Scientific and Research Publications*, vol. 6, no. 6, pp. 1-3, June 2013.

- [21]. A.S. Mohamad, M. Renlian, L.U. Xiqun, Li Wanyou, “Numerical Analysis And Experimental Evaluation Of Cylinder Liner Macro-Scale Surface Texturing”, in Proc. ASME Internal Combustion Engine Division Fall Technical Conference, vol. 2, pp. 1-9, Nov. 2015.
- [22]. H. Xianjun, R.F. Turkson, M.K.A. Ali, M. Ezzat “An analytical study of tribological parameters between piston ring and cylinder liner in internal combustion engines”, Journal of tribology, vol. 230, no. 4, pp. 329-349, Aug 2015.
- [23]. L. Jun, X. Youbai, Z. Zhang, “Design approach for optimization of a piston ring profile considering mixed lubrication”, Friction Springer, vol. 4 , no. 4, pp. 335-346, Dec. 2016.
- [24]. E.H. Smith, G.G.A. Fatjo, I.Sherrington, “Piston-ring film thickness: Theory and experiment compared”, Journal of Engineering Tribology, vol. 1, no. 1, pp. 1-8, March 2017.
- [25]. A. Razavykia , C. Delprete , "Piston ring–liner lubrication and tribological performance evaluation", J Engineering Tribology, vol. 232 ,no. 2, pp. 193-209, April 2017.

APPENDIX 1

$$\frac{d}{dx} \left(h^3 \frac{dp}{dx} \right) = 6\eta U \frac{dh}{dx} + 12\eta\omega \frac{\partial h}{\partial \theta}$$

Equating forces in x direction:

$$[p + \left(\frac{\partial p}{\partial x}\right)dx] dzdy + \tau dzd\tau - [\tau + \left(\frac{d\tau}{dy}\right)] dzdx - pdzdy = 0$$

$$\Rightarrow \frac{\partial p}{\partial x} = \frac{\partial \tau}{\partial z} \quad (1)$$

According to Newton's law of viscosity,

$$\tau = \eta \frac{\partial u}{\partial z}$$

Therefore equation (1) becomes

$$\frac{\partial p}{\partial x} = \eta \frac{\partial^2 u}{\partial z^2} \quad (2)$$

Similarly, for y direction,

$$\frac{dp}{dy} = \eta \frac{\partial^2 v}{\partial z^2} \quad (3)$$

Pressure gradients is negligible in Z-direction

$$\frac{dp}{dz} = 0 \quad (4)$$

Equation (2) can also be written as,

$$\frac{\partial^2 u}{\partial z^2} = \frac{1}{\eta} \frac{\partial p}{\partial x}$$

Integrating above equation twice with respect to x

$$\frac{\partial u}{\partial z} = \frac{1}{\eta} \frac{dp}{dx} z + C_1$$

$$u = \frac{1}{2\eta} \frac{dp}{dx} z^2 + C_1 z + C_2 \quad (4)$$

Assuming “no slip” condition, we have boundary conditions as,

$$\text{At } z=0, u=0$$

$$\text{At } z=h, u=U$$

Putting above Boundary Conditions in equation (4),

$$c_1 = \frac{U}{h} - \frac{1}{2\eta} \frac{dp}{dx} h$$

$$c_2 = 0$$

Equation (4) can be written as:

$$u = \frac{1}{2\eta} \frac{dp}{dx} (z^2 - hz) + \frac{U}{h} z \quad (5)$$

similarly for y direction, we have,

$$v = \frac{1}{2\eta} \frac{\partial p}{\partial y} (z^2 - hz) + \frac{V}{h} z \quad (6)$$

Considering general form of the continuity equation;

$$\frac{\partial}{\partial x} (\rho u) + \frac{\partial}{\partial y} (\rho v) + \frac{\partial}{\partial z} (\rho w) + \frac{\partial \rho}{\partial t} = 0 \quad (7)$$

Integrating the continuity equation with respect to z across the fluid film thickness h between the piston ring and cylinder liner;

$$\int_0^h \frac{\partial(\rho u)}{\partial x} dz + \int_0^h \frac{\partial(\rho v)}{\partial y} dz + \int_0^h \frac{\partial(\rho w)}{\partial z} dz + \int_0^h \frac{\partial \rho}{\partial t} dz = 0$$

$$\Rightarrow \int_0^h \frac{\partial(\rho u)}{\partial x} dz + \int_0^h \frac{\partial(\rho v)}{\partial y} dz + \rho w(h) + \frac{\partial \rho}{\partial t} h = 0$$

$$\text{But } w(h) = \frac{\partial h}{\partial t};$$

$$\Rightarrow \int_0^h \frac{\partial(\rho u)}{\partial x} dz + \int_0^h \frac{\partial(\rho v)}{\partial y} dz + \frac{\partial(\rho h)}{\partial t} = 0 \quad (8)$$

Now apply Leibnitz's rule for differentiating an integral,

$$\frac{\partial}{\partial x} \int_{a(t)}^{b(t)} f(x, t) dx = f[b(t), t] \frac{db}{dt} - f[a(t), t] \frac{da}{dt} + \int_{a(t)}^{b(t)} \frac{\partial f(x, t)}{\partial x} dx$$

Applying above operation on equation (8),

$$\Rightarrow \frac{\partial}{\partial x} \int_0^h \rho u dz + \frac{\partial}{\partial y} \int_0^h \rho v dz + \frac{\partial(\rho h)}{\partial t} = 0 \quad (9)$$

Since $\rho \neq \rho(z)$, therefore it can be removed from the integral.

Also ,

$$\begin{aligned} \int_0^h u dz &= \int_0^h \left(\frac{dp}{dx} (z^2 - hz) + \frac{U}{h} z \right) dz \\ \Rightarrow \int_0^h u dz &= \frac{1}{2\eta} \frac{\partial p}{\partial x} \left[\frac{h^3}{3} - \frac{h^3}{2} \right] + \frac{Uh}{2} \\ \Rightarrow \int_0^h u dz &= -\frac{1}{12\eta} \frac{\partial p}{\partial x} h^3 + \frac{Uh}{2} \end{aligned} \quad (10)$$

Similarly;

$$\int_0^h v dz = -\frac{1}{12\eta} \frac{\partial p}{\partial y} h^3 + \frac{Vh}{2} \quad (11)$$

Putting (10) & (11) in equation (9), we get,

$$\begin{aligned} \frac{\partial}{\partial x} \left[-\frac{1}{12\eta} \frac{\partial p}{\partial x} h^3 + \frac{Uh}{2} \right] + \frac{\partial}{\partial y} \left[-\frac{1}{12\eta} \frac{\partial p}{\partial x} h^3 + \frac{Vh}{2} \right] + \frac{\partial(\rho h)}{\partial t} &= 0 \\ \Rightarrow \frac{\partial}{\partial x} \left(\frac{1}{12\eta} \frac{\partial p}{\partial x} h^3 \right) + \frac{\partial}{\partial y} \left(\frac{1}{12\eta} \frac{\partial p}{\partial x} h^3 \right) &= \frac{\partial}{\partial x} \left(\frac{\rho Uh}{2} \right) + \frac{\partial}{\partial y} \left(\frac{\rho Vh}{2} \right) + \frac{\partial(\rho h)}{\partial t} \end{aligned}$$

$$\Rightarrow \frac{\partial}{\partial x} \left(\frac{\rho h^3}{\eta} \frac{\partial p}{\partial x} \right) + \frac{\partial}{\partial y} \left(\frac{\rho h^3}{\eta} \frac{\partial p}{\partial y} \right) = 6 \left[\frac{\partial}{\partial x} (\rho U h) + \frac{\partial}{\partial y} (\rho V h) \right] + 12 \eta \frac{\partial}{\partial t} (\rho h)$$

Since we have assumed incompressible fluid with constant viscosity η , therefore above equation becomes,

$$\Rightarrow \frac{\partial}{\partial x} \left(h^3 \frac{\partial p}{\partial x} \right) + \frac{\partial}{\partial y} \left(h^3 \frac{\partial p}{\partial y} \right) = 6 \eta \left[U \frac{\partial h}{\partial x} + V \frac{\partial h}{\partial y} \right] + 12 \frac{\partial h}{\partial t}$$

Here we are having one Dimensional Observation Therefore above equation reduces to,

$$\Rightarrow \frac{\partial}{\partial x} \left(h^3 \frac{\partial p}{\partial x} \right) = 6 \eta U \frac{\partial h}{\partial x} + 12 \eta \frac{\partial h}{\partial t} \quad (12)$$

APPENDIX 2

Matlab Codes

Generate and plot elliptical profile

```

%%generate and plot elliptical profile%%

t=linspace(-2,2,100)      %span over which elliptical profile is considered%
x=t'
v=x.^2
c=1
b=4                      %total distance over which elliptical profile is assumed or width of
piston ring%
h=1*10^-3                %minimum oil film thickness%
g=size(v)
y2=max(g)
y2=zeros(y2,1)
y2=(c*(sqrt((1-(4*v/(b^2)))))))+h %equation for elliptical profile%
plot(x,y2)

```

Generate parabolic profile over the required span

```

%% generate parabolic profile over the required span%%

t=linspace(-2,2,100)      %span over which parabolic profile is considered%
x=t'
v=x.^2
c=1
b=4                      %total distance over which elliptical profile is assumed%
h=1*10^-3
g=size(v)
y1=max(g)
y1=zeros(y1,1)
y1=((4*c*v)/b^2)+h        %parabolic curve equation%
plot(x,y1)

```

Obtain parabolic and elliptical profile on same graph

```

%% obtain parabolic and elliptical profile on same graph%%

%parabolic profile%
t=linspace(-2,2,100)    %span over which parabolic profile is considered%
x=t'
v=x.^2
c=1
b=4                    %total distance over which elliptical profile is assumed%
h=1*10^-3             %minimum oil film thickness%
g=size(v)
y1=max(g)
y1=zeros(y1,1)
y1=((4*c*v)/b^2)+h    %parabolic curve equation%
plot(x,y1)

hold on

%elliptical profile%
t=linspace(-2,2,100)    %span over which elliptical profile is considered%
x=t'
v=x.^2
c=1
b=4                    %total distance over which elliptical profile is assumed%
h=1*10^-3             %minimum oil film thickness%
g=size(v)
y2=max(g)

```

```
y2=zeros(y2,1)
y2=(c*(sqrt((1-(4*v/(b^2)))))))+h %elliptical curve equation%
plot(x,y2)
hold off
```

Merge elliptical and parabolic profile over a span

```
%%merge elliptical and parabolic profile over a span%%
x=[-2.0000
-1.9596
-1.9192
-1.8788
-1.8384
-1.7980
-1.7576
-1.7172
-1.6768
-1.6364
-1.5960
-1.5556
-1.5556
-1.5152
-1.4747
-1.4343
-1.3939
-1.3535
-1.3131
-1.2727
-1.2323
-1.1919
```

-1.1515
-1.1111
-1.0707
-1.0303
-0.9899
-0.9495
-0.9091
-0.8687
-0.8283
-0.7879
-0.7475
-0.7071
-0.6667
-0.6263
-0.5859
-0.5455
-0.5051
-0.4646
-0.4242
-0.3838
-0.3434
-0.3030
-0.2626
-0.2222
-0.1818
-0.1414
-0.1010
-0.0606
-0.0202
0.0202
0.0606

0.1010
0.1414
0.1818
0.2222
0.2626
0.3030
0.3434
0.3838
0.4242
0.4646
0.5051
0.5455
0.5859
0.6263
0.6667
0.7071
0.7475
0.7879
0.8283
0.8687
0.9091
0.9495
0.9899
1.0303
1.0707
1.1111
1.1515
1.1919
1.2323
1.2727
1.3131

1.3535
1.3939
1.4343
1.4747
1.5152
1.5556
1.5556
1.5960
1.6364
1.6768
1.7172
1.7576
1.7980
1.8384
1.8788
1.9192
1.9596
2.0000]'

y=[1.0010
0.9610
0.9218
0.8835
0.8459
0.8092
0.7733
0.7382
0.7039
0.6704
0.6378

0.6059

0.6295

0.6537

0.6765

0.6979

0.7181

0.7372

0.7553

0.7724

0.7886

0.8040

0.8186

0.8325

0.8456

0.8581

0.8699

0.8811

0.8917

0.9017

0.9112

0.9201

0.9285

0.9364

0.9438

0.9507

0.9571

0.9631

0.9686

0.9736

0.9782

0.9824

0.9861

0.9895

0.9923

0.9948

0.9969

0.9985

0.9997

1.0005

1.0009

1.0009

1.0005

0.9997

0.9985

0.9969

0.9948

0.9923

0.9895

0.9861

0.9824

0.9782

0.9736

0.9686

0.9631

0.9571

0.9507

0.9438

0.9364

0.9285

0.9201

0.9112

0.9017

0.8917
0.8811
0.8699
0.8581
0.8456
0.8325
0.8186
0.8040
0.7886
0.7724
0.7553
0.7372
0.7181
0.6979
0.6765
0.6537
0.6295
0.6059
0.6378
0.6704
0.7039
0.7382
0.7733
0.8092
0.8459
0.8835
0.9218
0.9610
1.0010]'

plot(x,y)

```

p=polyfit(x,y,4)
hold on

f = polyval(p,x)
table = [x f y-f]
plot(x,y,x,f,'-')
hold off

```

Plot graph for angle turned by crank v/s fluid film thickness

```

%%Plot graph for angle turned by crank v/s fluid film thickness%%
t=-2*pi:2*pi %angle of revolution of crank%
pi=180
r=55 %crank radius in mm%
n=4.25 %connecting rod to crank length ratio%
x=r*((1-cosd(t))+(n-(n.^2 - ((sind(t)).^2).^0.5)))) %displacement of piston%
y=[0.0682*x.^4 - 0.2951*x.^3 + 1.041 ]*10e-9 %equation of fluid film thickness%
plot(t,y)

```

Curve for total pressure in film and its variation v/s theta

```

clf
theta=0:10:360; %angle of revolution of crank%
r=55; %radius of crank%
n=4.25 %ratio of connecting rod to crank radius%
syms x A;

val1=3.271*1000; % Value of 6nU. . . . .
val2=12.45481*1000; % Value of 12nw. . . . .

```

```

h= (0.0682*x.^4-0.2951*x.^3+1.041)

first=int(1/h^2,x); %First integral term in the equation

second=int(x/h^3,x); %Second Integral term in the equation

third= int(1/h^3,x); %Third Integral term in the equation

fourth=((0.2728*x.^3)-(0.5902*x))

fifth=55*(sind(theta))+(((sind(2*theta))./(2*((18.0625-((sind(theta)).^2))).^(1/2))))

y=r*((1-cosd(theta))+(n-sqrt(square(n)-((sind(theta)).^2)))) %displacement of piston in
terms of theta%

fourth=subs(fourth,(x),(y))

sixth=fourth.*fifth

h=subs(h,(x),(y))

plot(theta,h)
title('Graph of h from 0 to 2pi')

first=subs(first,(x),(y))
second=subs(second,(x),(y))

```

```
third=subs(third,(x),(y))

first=double(first)
second=double(second)
third=double(third)
sixth=double(sixth)

totalvalue=(val1)*first+val2*sixth.*second+third
totalvalue=double(totalvalue)
figure(2)
plot(theta,totalvalue)
title('The Formula output after calculation')
```